THE UNIVERSITY OF TOKYO

# ACCURATE AND EFFICIENT NODE LOCALIZATION IN WIRELESS SENSOR NETWORKS

by

HONGYANG CHEN

A thesis submitted in partial fulfillment for the
degree of Doctor of Philosophy

in the

Graduate School of Information Science and Technology
Department of Information & Communication Engineering

February 2011

*Never leave that until tomorrow, which you can do today.*

Benjamin Franklin, American president

THE UNIVERSITY OF TOKYO

# *Abstract*

Graduate School of Information Science and Technology
Department of Information & Communication Engineering

Doctor of Philosophy

by HONGYANG CHEN

Localization algorithms for wireless sensor networks (WSNs) have been designed to find per-node location information, which is a key requirement in many applications of WSNs. Generally speaking, based on the type of information required for positioning, protocols can be divided into two categories: (i) range-based and (ii) range-free protocols. In this thesis, we focus on the investigation of localization algorithms for traditional WSNs, mobility-assisted WSNs, mobile sensor network, and wireless underground sensor networks.

In this thesis, we study the node localization problem in wireless sensor networks. Based on the statistical signal processing technology, several novel algorithms are proposed. Both range-based and range-free protocols are studied in the thesis. For range-free localization, we proposed a radical line based algorithm using the radio range of sensor nodes. With a slight increase in computations, this method provides a more accurate range-free localization based on the radical line of intersecting circles. Furthermore, a cooperative localization algorithm is proposed that considers the existence of obstacles in mobility-assisted wireless sensor networks (WSNs). This method is also a range-free method. An optimal movement scheduling method with mobile elements (MEs) is proposed to address limitations of static WSNs in node localization. For achieving high localization accuracy and coverage, a novel convex position estimation algorithm is proposed, which can effectively solve the problem when infeasible points occur because of the effects of radio irregularity and obstacles. For mobile sensor network and wireless underground sensor network, we propose the related algorithms which achieve high accuracy. It is more difficult to obtain the time-difference-of-arrival (TDOA) measurements in WUSNs than in terrestrial wireless sensor networks because of the unfavorable channel characteristics in the underground environment. In our thesis, the robust Chinese remainder theorem (RCRT) is used to robustly estimate TDOA or range difference in WUSNs and therefore improves the ranging accuracy in such networks. After obtaining the range difference, distributed source localization algorithms based on a diffusion strategy are proposed to decrease the communication cost while satisfying the localization accuracy requirement. This distributed source localization method is a range-based method for WUSNs.

# *Acknowledgements*

I could never have completed this work without the support and assistance of many people. First and foremost, I would like to express deepest gratitude to my advisor, Prof. Kaoru Sezaki, for his excellent guidance, valuable suggestions, and kind encouragement in academic. With his help, I learned how to define research problems and formalize them; how to design solutions and improve them; and how to write papers and present them. I also would like to thank Prof. H. Vincent Poor from Princeton University. His insight and passion for the research teaches me how to face and overcome difficulties and setbacks, and helps me grow as a researcher with a positive and optimistic view of life. For his consistent and generous support, I thank him from the bottom of my heart.

I also would like to express grateful thank to Prof. Ali. H. Sayed, Prof. Y.T. Chan, Dr. H.C. So, and Dr. Kenneth W.K. Lui for their kind advices, helpful assistance, technical support and countless hours of useful discussion on the direction and many issues regarding to my research. I would appreciate the final defense committee members, Prof. Toru Asami, Prof. Hiroshi Esaki, Prof. Shuichi Sakai, Dr. Yoshihiro Kawahara, and Dr. Masashi Toyoda, for their valuable comments and suggestions to my work.

This thesis would not have been possible without generous financial support from Japanese Government (Monbukagakusho) Scholarship program. Through its very kind staffs, Monbukagakusho also provides student accommodation and other convenient life supports. These supports are gratefully acknowledged.

It is very lucky for me to cooperate with my friends Qingjiang Shi, Rui Tan, Gang Wang, Zizhuo Wang, Pei Huang, and Bin Liu to name a select few. I also want to thank all colleagues at Sezaki Laboratory who have offered me friendship, insightful comments, ideas, and helpful discussions during the course of my study. I also would like to thank my friends Yanhui Gu, Jianjun Yang, Meirong Guo, Kai Wu, and Chen Wang. Without them, my life in Japan will not be so happy and harmonious.

Finally, all this would have not been worthwhile, but for my family. It is impossible to put into words my feelings of love and gratitude for my parents. It is their understanding, perpetual support, and unconditional love that make me overcome all the difficulties through all the years of my study in Japan.

# Contents

# List of Figures

# List of Tables

# Chapter 1

# Introduction

Recent advances in wireless communications and micro electro-mechanical system (MEMS) technologies have enabled the development of low-cost, low-power and small size wireless sensor nodes. Wireless sensor networks (WSNs) have become the current hot spot of networking area and have been used for various applications, such as oceanic resource exploration, pollution monitoring, tsunami warnings and mine reconnaissance. For all these applications, it is essential to know the locations of the data. Localization algorithms for wireless sensor networks (WSNs) have been designed to find per-node location information, which is a key requirement in many applications of WSNs.

## 1.1 Challenges for Network Localization

Localization plays a important role in many sensor network applications, however, itself is a difficult problem to be solved, because of the demanding requirements for low cost, high energy efficiency, and the scalable for the change of network size, as well as practical issues associated with node deployments. Herein, we summarize some major challenges we meet to design accurate and efficient node localization in wireless sensor networks.

*Distributed and Energy Efficient* The algorithm should be distributed. It can be robust to the case when the central node is dead. The algorithm should be with less traffic and power consumption. The requirement of less power consumption prohibits the use of special hardware.

*Infrastructure Less Environment* Sensor networks are normally deployed in some special areas. In these areas, infrastructure are less, such as base station from mobile phone network or radio signals from wireless AP towers. Hence, the designed algorithms should be autonomic without human calibration and extensive environment profiling.

Realizing the challenges for network localization, this dissertation aims to study the localization problem in sensor networks. We try to study the practical problem to find the tradeoff between the accuracy and energy cost for achieving excellent localization algorithms in sensor networks.

## 1.2 Motivation

A lot of localization algorithms have been proposed in this area. Generally speaking, based on the type of information required for positioning, protocols can be divided into two categories: (i) range-based and (ii) range-free protocols. Some ranging techniques that are available for localization include angle-of-arrival (AOA), received signal strength indicator (RSSI), time-of-arrival (TOA) and time-difference-of-arrival (TDOA) schemes. On the other hand, we may adopt range-free approaches in which one can find the positions of non-anchor nodes by calculating their distances from the designated but sparse anchor nodes with known positions, also known as landmarks. Due to the hardware limitations and power constraints of sensor nodes, solutions of range-free localization are often more preferable and can be considered as cost-effective options in some scenario where the higher localization accuracy is not strictly required.

Furthermore, the WSN connectivity and topology are subject to changes due to node addition and failure, irregular environment as well as node mobility. It is also important to address the negative effect from non-line-of-sight measurements, which occur when direct signal transmission paths between sensor pairs are blocked, because they will include large errors for node localization.

It is still a difficult problem to find an accurate and efficient localization algorithm in sensor networks. Hence, this thesis consider self-configuration and self-monitoring problem of estimating the position of unknown-position sensors with higher accuracy and lower power consumption using the information from anchor nodes. In this thesis, we study the node localization problem in wireless sensor networks from both range-based and range-free methods. Some statistical signal processing technology and optimization theory are applied in the thesis. Based on the statistical signal processing technology, several novel algorithms are proposed. In the thesis, we focus on both range-free and range-based techniques to study the benefits from both two techniques. We find it is a good idea to combine range-free and range-based methods together to address the node localization problem in the future. For range-free localization in static sensor network, we proposed a radical line based algorithm using the radio range of sensor nodes. With a slight increase in computations, this method provides a more accurate range-free localization based on the radical line of intersecting circles. Furthermore, a cooperative localization algorithm is proposed that considers the existence of obstacles in mobility-assisted wireless sensor networks (WSNs), which is also a range-free based method. An optimal movement scheduling method with mobile elements (MEs) is proposed to address limitations of static WSNs in

node localization. In this scheme, a mobile anchor node cooperates with static sensor nodes and moves actively to refine location performance. It takes advantage of cooperation between MEs and static sensors while, at the same time, taking into account the relay node availability to make the best use of beacon signals and address the effect of obstacle. For achieving high localization accuracy and coverage, a novel convex position estimation algorithm is proposed, which can effectively solve the problem when infeasible points occur because of the effects of radio irregularity and obstacles. This method is the only range-free based convex method to solve the localization problem when the feasible set of localization inequalities is empty. Simulation results demonstrate the effectiveness of this algorithm. For mobile sensor network and wireless underground sensor network, we propose the related algorithms which achieve high accuracy. For mobile sensor network, all anchors and sensors are moving, which is different the case with only one mobile anchor. In mobile sensor network, it is more complicated and the particle filter technology is used in this scenario. In some special application areas, the localization algorithm meets special requirement and the related challenges. Hence, we discuss the localization problem in wireless underground sensor networks. It is more difficult to obtain the time-difference-of-arrival (TDOA) measurements in WUSNs than in terrestrial wireless sensor networks because of the unfavorable channel characteristics in the underground environment. The robust Chinese remainder theorem (RCRT) has been shown to be an effective tool for solving the phase ambiguity problem and frequency estimation problem in wireless sensor networks. In our thesis, the RCRT is used to robustly estimate TDOA or range difference in WUSNs and therefore improves the ranging accuracy in such networks. After obtaining the range difference, distributed source localization algorithms based on a diffusion strategy are proposed to decrease the communication cost while satisfying the localization accuracy requirement.

As we completed this work, we are happy to find localization attracts a lot of attention and plays important role for the application of WSNs. However, it is still a tough problem to be addressed well. We have done some work to find the gap between the accuracy and efficiency for node localization. It is still an interesting topic to investigate and propose hybrid solutions so as to leverage the advantages of both range-based and range-free types. The close error bound for range-free algorithms are still opened. Furthermore, based on the derived error bound, to derive the optimal anchor placement is another interesting problem under our consideration.

## 1.3 Main Contributions

This thesis makes contributions to both range-based and range-free localization techniques. The main target is to design localization algorithms with high accuracy and energy efficiency. As shown in Fig. 1.1, we show an overview of the main work for this thesis. The main contributions of this thesis can be summarized as follows:

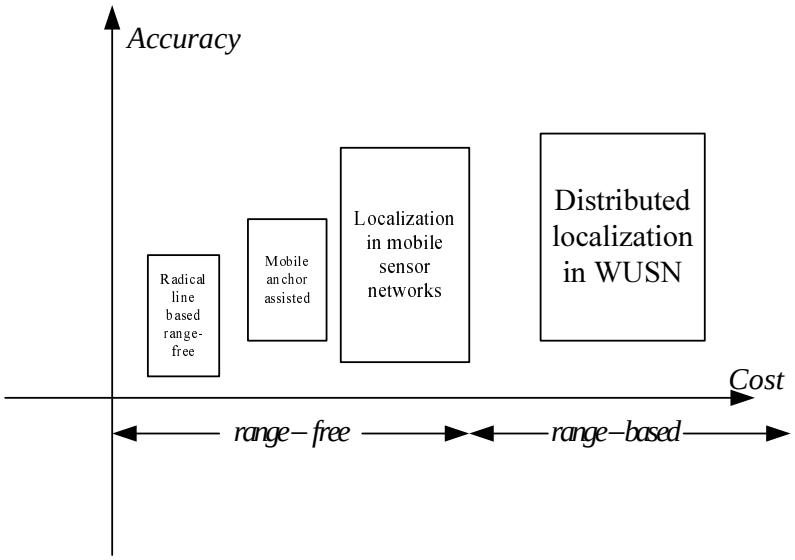


FIGURE 1.1: Overview on the main work of the thesis

- We present a range-free localization technique based on the radical line of intersecting circles. The intersection of radical lines is normally within the common region of the circles constructed by anchors. It is the basic idea to improve the localization accuracy against the shortcoming of the traditional centroid method. When there are more than three anchors in range, we select two anchors and use them only to significantly decrease the computational cost. This technique provides greater accuracy than the centroid algorithm, at the expense of a slight increase in computational load. Simulation results show that for the scenarios studied, the radical line method can give an approximately 2 to 30% increase in accuracy over the centroid algorithm, depending on whether or not the anchors have identical ranges, and on the value of DOI.

- We present a new cooperative localization scheme that can achieve high localization accuracy in mobility-assisted wireless sensor networks when obstacles exist. Considering the complex localization scenario, namely, the feasible set is empty, a convex localization algorithm has been presented to address the effects of non-ideal transmission of radio signals. We have developed an optimal movement schedule for MEs that can achieve a shortest path under expected localization accuracy. To address the effect of obstacle, the optimal relay node is selected to transmit the beacon signal to the unknown-position nodes within the special area of obstacle. It has been shown in the simulation results that the proposed cooperative localization scheme can achieve high localization accuracy by including a mobile element.

- We present a distributed hop distance measurement and particle filter-based cooperative localization algorithm for mobile WSNs. Our proposal is scalable, robust, and self-adaptive to the dynamics of a mobile sensor network. Our proposed algorithm can reduce the hop distance estimation error accumulated over multiple hops by using a differential error correction scheme. In order to efficiently suppress redundant broadcasts and to reduce communication overhead, a backoff-based broadcast mechanism is proposed. It also improves localization performance by including particle filtering technology. Simulation results show that the proposed algorithm achieves better performance than other state-of-the-art algorithms.

- We present energy efficient localization schemes that can achieve high localization accuracy in wireless underground sensor networks. These distributed localization algorithms require low computational complexity and energy consumption based on a diffusion strategy. An accurate RCRT based ranging scheme using TDOA to determine range differences between sensors and source that does not require time synchronization is also proposed. We notice that the TDOA can usually be obtained from the measurement of a signals phase which is susceptible to phase ambiguity problems in WUSN. The Chinese remainder theorem (CRT) offers a closed-form analytical algorithm to calculate a dividend from several of its corresponding divisors and remainders, and can be applied to solve the ambiguity problem here. It has been shown via simulation results that the proposed localization algorithms achieve excellent localization accuracy with lower communication cost.

## 1.4 Thesis Outline

The rest of this thesis is organized as follows.

Chapter 2 introduces some related work, including range-based localization, range-free localization and node localization in mobile sensor network.

In Chapter 3, we propose a range-free localization algorithm based on the radical line.

In Chapter 4 we study node localization in mobility-assisted sensor network. One mobile element is included to improve the localization performance. The optimal moving trace for mobile element is also derived.

In Chapter 5, we propose a localization algorithm for mobile sensor network. Different with previous work, in this scenario, all of the nodes are moving. It is more difficult to estimate node position accurately.

In Chapter 6, a distributed source localization algorithm for wireless underground sensor network is proposed.

# Chapter 2

# Localization Measurements and Algorithms

Making sensing data geographically meaningful, location information plays important role for many applications of WSN, and a lot network functions can be helped based on the location information, including network routing, topology control, coverage, boundary detection, clustering, etc. In this chapter, we study a large number of existing localization approaches with focuses on error control and energy efficient, the two important factors to evaluate the performance of a localization algorithm. With summarizing the related works in this area, we can easily to understand the state-of-the-art. The limitations for previous works are also pointed out in the chapter. Then, the reason why we focus on some algorithms in this thesis is introduced as well.

This chapter reviews measurements widely used in WSN and the selected publications related to the topics on localization algorithm in wireless sensor networks. Both range-based and range-free algorithms and the case node with mobility ability are introduced. In Section 2.1, measurements used in WSN localization are introduced. In Section 2.2, we summarize current research works on range-based localization. In Section 2.3, we introduce range-free localization. Finally, Section 2.4 presents localization algorithms in mobile sensor networks.

## 2.1 Measurements

Pair-wise measurements plays important role to develop reliable localization systems in WSN. However, it is difficult to accurately obtain the measurements since the wireless channel between pair-wise nodes is affected by obstructions, reflectors, people and objects in motion.

Time of arrival (TOA), time difference of arrival (TDOA), received signal strength, and angle of arrival (AOA) are widely used measurements to achieve location estimation in wireless networks. Although received signal strength (RSS) measurements are easily available, but the major drawback of the method is that multi-path reflections, non line-of-sight conditions, and other shadowing effects might lead to erroneous distance estimates. Angle of arrival (AOA) measurements is an attractive method due to the simplicity of subsequent calculations (triangulation). But the main drawback of this technique for terrestrial systems is the possibility of error in estimating the directions caused by multi-path reflections. Time-of-arrival and time-difference-of-arrival (TOA, TDOA) measurements: which may be used to estimate the distance from a set of reference points by measuring the propagation times (or differences there of) of signals. TOA has a disadvantage compared to TDOA as processing delays and non-LOS propagation can introduce errors.

The measurement model is important to obtain accurate measurements. Obstacle can affect the measurement significantly. Normally, some distribution for measurement error and non-line-of-sight error are assumed. However, depending on the different environments, the actual distributions are very difficult to obtain. That is the main error for localization. Some works have done several measurement experiments in order to determine accurate statistical models for RSS and TOA measurements in indoor wireless sensor networks. It is still an open problem to find more accurate measurement model or use some physical features to improve the performance.

## 2.2 Range-based Localization

Range-based protocols estimate absolute point-to-point distance to calculate the location between neighboring sensors. Range-based algorithms are typically based on angle-of-arrival (AOA), RSSI [40], time-of-arrival (TOA) or time-difference-of-arrival (TDOA) measurements. A promising technology is the ultra wideband (UWB) technology where precise ranging can be embedded into data communication.

Recent work demonstrated that the sensing performance of WSNs can be improved by using mobility capability node. Xing *et al.* [60] study target detection for mobility-assisted WSNs. They exploited reactive mobility to improve the target detection performance of WSNs. In their approach, mobile sensors collaborate with static sensors and move reactively to achieve the required detection performance. Wang *et al.* [55] used Voronoi diagrams to detect the coverage holes and devised three movement-assisted sensor deployment protocols based on the principle of moving sensors from densely deployed areas to sparsely deployed areas. Wang *et al.* [54] presented a mobility-assisted network for field coverage which can be remarkably improved by integrating a small set of mobile sensors. They offered an optimal algorithm to calculate

the coverage contributions, which explores the potentials of the mobile sensors and extends the network lifetime.

Several studies exploited the effect of mobile nodes on node localization for WSNs. In these methods, a small number of mobile devices referred to as MAs roam about sensing fields and assist to improve localization performance. Luo *et al.* [31] proposed a TDOA localization algorithm for movement-assisted sensor networks. A mobile beacon is used to measure the mobility-differentiated TOA in [31], which will increase mobile beacon's communication cost. Based on the RF-based technology, [62] presented three algorithms for tracking transceiver-free moving objects in an indoor WSN.

RSSI has been widely used as a distance measure in the context of static WSNs because of its simplicity. The impact of a number of parameters, such as the operating frequency, the transmitter–receiver distance, the variation of transceivers, the antenna orientation, and the environment, on (received signal strength) RSS measurements were investigated using Tmote Sky nodes in real outdoor environments [48].

After studying the exist range-based algorithms, we can see that radio, UWB, and acoustic signals are the most investigated technologies for range-based localization in wireless sensor networks. However, for UWB and acoustic signals, the communication range is limited although can achieve higher ranging performance. For radio signal, the radio range is large but also relies on the hardware which increases the cost for a sensor node. TOA-based range errors in multipath or non-line-of-sight environments can be greater than those caused by additive noise alone. In a word, range-based method can achieve higher accuracy but also including higher cost and energy consumption. In wireless underground sensor networks, it is difficult to accurately obtain the ranging information. Thus, we use robust Chinese remaind theorem to improve the ranging performance. To decrease the energy consumption, a distributed source localization is proposed in this thesis based on the diffusion strategy.

## 2.3 Range-free Localization

Vivekanandan *et al.* [52] proposed a concentric anchor beacon (CAB) localization algorithm for WSNs. In the CAB approach, each anchor node emits beacon signals at different transmission power levels to constrain the node to be localized to a small intersection area. After receiving the beacon signals, a node can determine in which annular ring it is located within each anchor node and uses the geometric center of the intersection of the rings as its position estimate. Ssu *et al.* [46] proposed a range-free localization scheme using mobile anchor points. In order to reduce the impact of obstacles, an enhanced beacon point selection method is proposed in their approach. Xiao *et al.* [59] proposed a distributed algorithm for locating sensor nodes using

a single mobile beacon. Three beacon movement strategies and their impacts on localization performance were studied. However, their algorithm considers only one mobile beacon and hence fails to exploit the cooperation among multiple mobile beacons. Moreover, in order to achieve high localization accuracy in their algorithm, the moving step of the mobile anchor becomes quite small, which in turn requires frequent broadcasting and consequent higher power consumption.

DV-Hop [35], MDS-MAP [39], RPA [37], Amorphous [34], which are based on the network connectivity information, proposed using local neighborhood sensing to calculate hop-based virtual distances for large-scale sensor network localization. In those systems, only a small number of anchors are necessary for constructing the global coordinates, which significantly reduces the system cost. The problems of "holes" and "complex shapes" , caused from the practical irregular node deployment with obstacles have been studied in [27] [53] [24]. However, we found that localization by means of connectivity alone does not make full use of information available from local neighborhood sensing. Recently, event-driven methods such as Lighthouse [36], Spotlight [47] and etc., have been recognized as another important branch of range-free localization, in which localization events embedding temporal and spatial relationships are generated and distributed across the network area for determining nodes positions. Although event driven localization provides tradeoffs between localization accuracy and system cost, generating localization events may not be easy and convenient in some scenarios. MDS-MAP [39] is a popular range-free method which is based on multidimensional scaling (MDS), a data analysis technique that takes $O(n^3)$ time for a network of $n$ nodes. The method first derives a relative map of the network and then transform it to absolute coordinates if anchors are available. It has been shown in [39] that the MDS–MAP method always outperforms all previously mentioned range–free methods but [18] when the network is relatively uniform with *few anchors*. In [18], Geogetti *et al.* propose a neural network (self–organizing map, SOM) based method, which, compared to the MDS–MAP method, can offer better performance for networks with low connectivity level ($< 10$) and comparable performance for those with higher connectivity level. Therefore, we use the MDS–MAP method for direct comparison in our simulations, where all tested networks are assumed of relatively high connectivity level in 2-D space (generalization to 3-D networks is easy). However, A drawback of MDS–MAP is that the anchors' position are only used for absolute coordinates transformation from relative map rather than relative map generation but which is central to MDS–MAP. It is because of this drawback that the method works nicely when there are few or no anchors, but not as well when there are more anchors (especially when a number of "virtual anchors" can be generated by a mobile anchor).

Semidefinite programming (SDP) [6] has also been introduced and applied to sensor network localization. However, most of the proposed methods deal with the range-based sensor network localization problem, e.g., [41] [30] [3].

Normally, range-free localization algorithms based on network connectivity or anchor proximity achieve low overhead for communication and computation, but, its accuracy is not high. Centroid and APIT methods achieve good performance with lower energy consumption than range-based method. However, high anchor density is required to achieve higher accuracy. For DV-hop method, the performance is not good if the network topology is complicated, such as a concave area. Since in this area, it is difficult to obtain an accurate hop-distance. Another drawback for DV-hop is the requirement of flooding, which significantly increases the communication cost for the whole network. Hence, in this thesis, a more effective hop-distance is proposed. To reduce the communication cost, a back-off based method is applied in our localization algorithm for mobile sensor networks.

Some applications of wireless sensor networks involve stationary sensors. In the normally static WSN, a range-free method using radical line is proposed in the thesis. Different with the centroid or weighted centroid method, we rely on radical line to assure the estimate will within the common area of the circles constructed by anchors. It is the basic idea to increase the accuracy. In order to decrease the computational cost when there are more than 3 anchors in range, we propose a method to select only two anchors. This is an interesting point for the anchor selection since the increase number of anchors cannot always increase the localization accuracy as studied before. However, our radical line based method is still not an optimal solution. To find the optimal estimate for this kind of radio range based methods is a very interesting topic.

## 2.4 Localization in Mobile Sensor Networks

Several works have been proposed for mobile WSNs. MCL [22] is designed for mobile sensor networks based on the sequential Monte Carlo method. A range-based version of MCL has also been proposed [15], which combines range-based and range-free location information to reduce the estimation error. Baggio *et al.* [2] improve the Monte Carlo localization scheme by reducing the sample prediction area. Their work, called MCB, draws valid samples faster and reduces the number of iterations necessary to fill the sample set. Computation overhead is reduced by this mechanism, but it still depends on specific parameters such as the fixed radio transmission range. Hsieh *et al.* [21] have proposed a localization algorithm which dynamically updates and makes use of reference information for cost-efficiency, and has a feasible solution for nodes receiving insufficient anchor information.

Depending on the anchor density of a network, there will be occasions when a regular node will not communicate with any anchor, which undermines the localization process. One idea to avoid the lack of coverage is to also allow regular nodes to participate in the cooperative localization process. While MCL uses anchor information only in the filtering stage, we also can apply it to constrain the area from which the samples are drawn in the prediction stage. As

a result, sampling efficiency is increased, as less samples are rejected by the filtering process, saving node's energy. Based on these two possible directions, we derive a localization algorithm for mobile sensor networks.

Different from the former work on localization algorithms for mobile WSNs, we study the cooperation between neighbor nodes that achieve high localization performance. Our scheme belongs to the range-free category of localization algorithms. Our approach differs from the above mentioned works in three significant ways: first, different from DV-Hop [35] and Gradient [34], which are based on simple flooding mechanism, we propose a backoff-based flooding to efficiently suppress redundant broadcasts and reduce communication overhead. For the hop distance measurement, a differential error correction scheme is devised to reduce the measurement error accumulated over multiple hops for the average hop distance. Second, our approach draws a more effective particle prediction area, borrowing some ideas from MCB, based on the positions of virtual anchor nodes, created with the active cooperation between regular nodes and its neighbors. Third, the sensor information is used to reduce even more the prediction area, thus reducing the estimation error of the non-anchor nodes. Furthermore, our approach does not require previous knowledge of the radio transmission range for filtering.

# Chapter 3

# Range-free Localization with the Radical Line

A wireless sensor network (WSN) [19] typically consists of anchors and sensors communicating with each other. An anchor broadcasts its position coordinates, together with operating instructions, to the sensors. A sensor needs to determine its position to report to the anchors. Position determination can come from time-of-arrival, time-difference-of-arrival or angle-of-arrival measurements [31]. But when the sensors are low cost, low power and expandable units, with limited resources for computation, they often rely on range-free (RF) localization instead [8]. In this chapter, we propose a range-free localization algorithm based on the radical line for static sensor networks.

The rest of this chapter is organized as follows. In Section 3.1 we introduce the background of radical line based range-free localization. Section 3.2 gives the development of the RL algorithm (RLA). Section 3.3 contains simulation results, which show that the RLA is more accurate than the CA, especially when the radii $R_i$ are different. Conclusions are given in Section 3.4.

## 3.1 Introduction

In RF localization, a sensor $P$ determines its unknown position $P = [x, y]^T$ from $N$ in-contact anchors $a_i$ at known positions $a_i = [x_i, y_i]^T$ and having radio ranges $R_i, i = 1, ..., N$. The sensor position must satisfy

$$\begin{aligned} \|P - a_i\|^{1/2} &= [(x - x_i)^2 + (y - y_i)^2]^{1/2} \\ &\leqslant R_i, \qquad i = 1, 2, \ldots, N. \end{aligned} \tag{3.1}$$

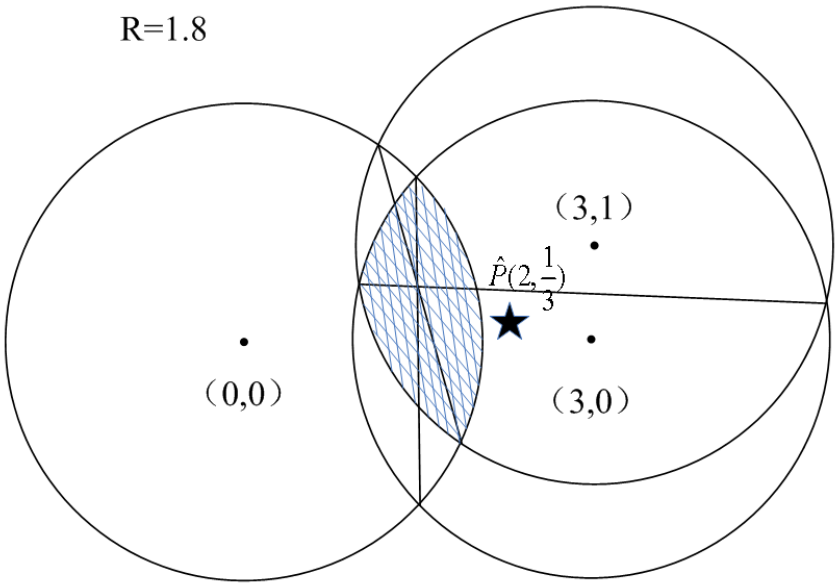


FIGURE 3.1: The CA and radical line solutions

Solving (3.1) requires nonlinear programming, and there is not a unique answer. The Centroid Algorithm (CA) [3] gives a simple estimate $\hat{P} = [\hat{x}, \hat{y}]^T$, where

$$\hat{x} = \frac{\sum_{i=1}^{N} x_i}{N} \quad and \quad \hat{y} = \frac{\sum_{i=1}^{N} y_i}{N}. \tag{3.2}$$

But $\hat{P}$ from (3.2) sometimes is outside the region of intersections (RI) of the circles centered at $a_i$ with radii $R$, as defined by (3.1). For example, the $\hat{P}$ in Fig. 3.1 is outside the RI (shaded area) of the three circles.

This paper proposes a new RF algorithm that has better accuracy than CA, but with a marginal increase in computations. However, the additional computations are well within the capability of present day sensors.

The line joining the intersection points of two circles is the radical line (RL) [13]. In Fig. 3.1, the RI contains a segment of the RL of any two circles, and the three RLs meet at a point inside the RI. Indeed, [13] proves that for three circles whose centers are not collinear, their three RLs always intersect at a point. Although sometimes this point can be outside the RI, it is inside in most cases.

## 3.2 The Radical Line Algorithm

In WSNs, a sensor can determine whether it is in the transmission range of an anchor node according to the beacon signal received from the anchor. Most literature on range-free localization assume a nominal range (or detection range) $R$, i.e., an anchor can communicate with a sensor within $R$ meters from it. However, the actual range in practice is dependent on the propagation conditions. A measure of the variation in range coverage is the degree of irregularity (DOI). Its value denotes the maximum range variation per unit degree change in the direction of radio propagation. Recently, [33] gives a condition required for a successful anchor-to-sensor contact. Let $W(a_i)$ be the power received by a sensor from $a_i$, $Q$ be the ambient noise power, and $S$ the interference power in the WSNs. Then there is a contact only if

$$\frac{W(a_i)}{Q+S} \geqslant TH, \tag{3.3}$$

where $TH$ is a hardware dependent threshold.

Let a sensor $P$ be at an unknown position $P = [x, y]^T$, in contact with $N$ anchors $a_i$ at known positions $a_i = [x_i, y_i]^T$ and having radio ranges $R_i$. Hence $P$ must lie in the RI of the $N$ circles, centered at $a_i$ with radii $R_i$. Depending on $N$, there are three cases to consider.

### 3.2.1 $N > 3$

For $N$ circles, there are $\frac{N!}{2!(N-2)!}$ RLs. To reduce computations, RLA selects only the RLs of the two circles whose centers are separated by the largest distance among the $N$ circles. The idea behind this choice is that the RL of these two circles will be the shortest, and hence their RL has the highest probability of appearing inside the RI of all the $N$ circles.

Let

$$d_{ij} = \left\|a_i - a_j\right\|^{1/2} = d_{ji}, \quad i, j = 1, \ldots, N \tag{3.4}$$

be the distance between the centers of $a_i$ and $a_j$ and let $d_{qk}$ be the maximum of the values in (3.4). For illustration simplicity, let $q = 1$, and $k = 2$. Referring to Fig. 3.2, the end points of the RL are $I_a = [x_a, y_a]^T$ and $I_b = [x_b, y_b]^T$, and $O = [x_o, y_o]^T$ is the intersection between the RL and the line joining $a_1$ and $a_2$.

Let

$$d_{o1} = \|O - a_1\|^{1/2} \tag{3.5}$$

and

$$d_{o2} = \|O - a_2\|^{1/2}. \tag{3.6}$$

It follows that

$$d_{o1}^2 + m^2 = R_1^2 \tag{3.7}$$

and

$$d_{o2}^2 + m^2 = R_2^2. \tag{3.8}$$

Subtracting (3.8) from (3.7) gives

$$2(x_2 - x_1)x_o + 2(y_2 - y_1)y_o = R_1^2 - R_2^2 + k_2 - k_1, \tag{3.9}$$

where

$$k_i = x_i^2 + y_i^2. \tag{3.10}$$

Further, equating the slopes of the $a_1$ to $O$ and $a_2$ to $a_1$ lines in Fig. 3.2 yields

$$\frac{y_2 - y_o}{x_2 - x_o} = \frac{y_2 - y_1}{x_2 - x_1}, \tag{3.11}$$

giving

$$(y_2 - y_1)x_o - (x_2 - x_1)y_o = x_2(y_2 - y_1) - y_2(x_2 - x_1). \tag{3.12}$$

Solving (3.9) and (3.12) then gives $O(x_o, y_o)$.

Let $d_{12} = D$. Then

$$R_1^2 - d_{o1}^2 = m^2 = R_2^2 - (D - d_{o1})^2, \tag{3.13}$$

so that

$$d_{o1} = \frac{R_1^2 - R_2^2 + D^2}{2D} \tag{3.14}$$

and

$$m = (R_1^2 - d_{o1}^2)^{1/2}. \tag{3.15}$$

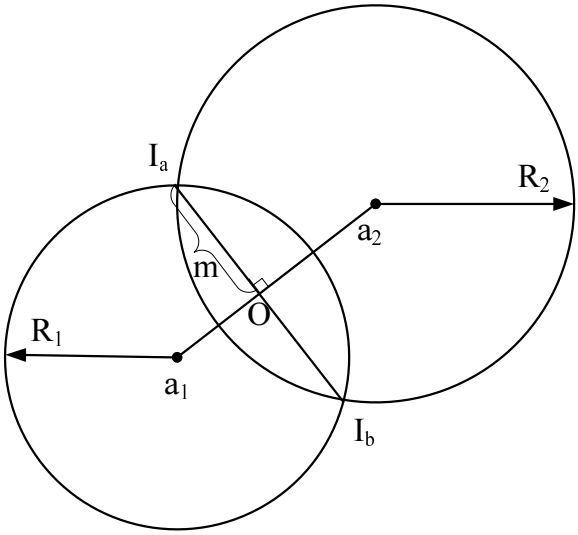


FIGURE 3.2: The end points of an RL

Now in Fig. 3.2, the following trigonometric relations hold:

$$\frac{x_o - x_a}{m} = \frac{y_o - y_1}{d_{o1}} \tag{3.16}$$

and

$$\frac{y_o - y_a}{m} = \frac{x_o - x_1}{d_{o1}}. \tag{3.17}$$

From (3.16) and (3.17), the coordinates for $I_a$ are

$$x_a = x_o - \frac{m}{d_{o1}}(y_o - y_1) \tag{3.18}$$

and

$$y_a = y_o + \frac{m}{d_{o1}}(x_o - x_1). \tag{3.19}$$

Following the same procedure gives

$$x_b = x_o + \frac{m}{d_{o1}}(y_o - y_1) \tag{3.20}$$

and

$$y_b = y_o - \frac{m}{d_{o1}}(x_o - x_1). \tag{3.21}$$

Next, RLA selects $L$ test points $t_l = [x_l, y_l]^T, \quad l = 1, \ldots, L$, on RL, by taking equal increments between $I_a$ and $I_b$ to give

$$x_l = x_a + \frac{l(x_b - x_a)}{L+1} \tag{3.22}$$

and

$$y_l = y_a + \frac{l(y_b - y_a)}{L+1}. \tag{3.23}$$

$L$ is a user parameter, depending on the resolution required. In the simulation experiment in Section 3.3, $L = 4$. At each $t_l$, RLA checks whether $t_l$ is inside the RI, and if not, how far away from the RI it is, by computing the error

$$\varepsilon_{li} = \|t_l - a_i\|^{1/2} - R_i = \begin{cases} \varepsilon_{li} & if\ \varepsilon_{li} > 0 \\ 0 & if\ \varepsilon_{li} \leqslant 0 \end{cases} \tag{3.24}$$

and then summing the errors over all $a_i$ to give

$$S_l = \sum_{i=1}^{N} \varepsilon_{li}. \tag{3.25}$$

If an $S_l = 0$, the corresponding $t_l$ is inside the RI and is the estimate for $P$. If all $S_l > 0$, the RL is not inside the RI of the $N$ circles. It is then necessary to compute the CA errors

$$S_c = \sum_{i=1}^{N} \varepsilon_{ci} \tag{3.26}$$

where $\varepsilon_{ci}$ comes from (3.24), with $c = [\hat{x}, \hat{y}]^T$ from (3.2) replacing $t_l$. The final estimate for $P$, $\hat{P}$, comes from choosing the $t_l$ or $c$, whose corresponding $S_l$ or $S_c$ is the minimum.

### 3.2.2 $N = 2$ and $N = 3$

When $N = 2$, $\hat{P}$ is the same as $O(x_o, y_o)$. When $N = 3$, RLA computes the intersection of the three RLs. Let that intersection point be $I = [x_I, y_I]^T$. Extending Fig. 3.2 to three circles yields

$$(x_I - x_i)^2 + (y_I - y_i)^2 + h^2 = R_i^2, \quad i = 1, 2, 3 \tag{3.27}$$

where $h^2 \leq m^2$. Subtracting this expression for $i = 2, 3$ from that for $i = 1$ results in

$$AI = b \tag{3.28}$$

where

$$A = \begin{bmatrix} x_2 - x_1 & y_2 - y_1 \\ x_3 - x_1 & y_3 - y_1 \end{bmatrix}, \tag{3.29}$$

$$and \;\; b = \frac{1}{2}\begin{bmatrix} k_2 - k_1 + R_1^2 - R_2^2 \\ k_3 - k_1 + R_1^2 - R_3^2 \end{bmatrix}. \tag{3.30}$$

Solving (3.28) gives

$$I = A^{-1}b. \tag{3.31}$$

If the determinant of $A$ equals 0, then the three circles are collinear. Or if $\|I - a_i\|^{1/2} > R_i$ for any $i$, then $I$ is outside the RI. For these two cases, RLA takes the centroid of the two circles with the largest separation as $\hat{P}$.

## 3.3 Simulation Results

In the simulation experiments, the WSN has an area of 100 m x 100 m, and contains 100 randomly placed (different for each trial) sensors. For a given number of anchors (NA), occupying random (different for each trial) but known positions, the number of anchors $N$ in contact with an arbitrary sensor can vary from 2 to NA. Some anchors have $R = R_{max} = 45m$, and some have $R = 0.5R_{max}$. The localization errors decrease with increasing NA. For 100 independent trials, the error as a fraction of $R_{max}$ is

$$e(NA) = \frac{1}{100}\sum_{j=1}^{100}\left\{\frac{\sum_{i=1}^{100}\left\|p_j(i) - \hat{p}_j(i)\right\|^{1/2}}{100R_{max}}\right\}. \tag{3.32}$$

In (3.32), $p_j(i)$ is the true $i$th sensor position at trial $j$, and $\hat{p}_j(i)$ is its estimate.

In an experiment where $DOI = 0$, a sensor that lies within the nominal $R_i$ of an anchor is in contact with that anchor. When $DOI \neq 0$, the actual $R_i$ is smaller, given by $R_i(DOI) = R_i(1 - DOI)$.

Fig. 3.3 is a snapshot of one trial in the anchor-sensor geometry with $NA = 30$ and different transmission ranges, together with the placement of $\hat{P}$. A dotted line joins $P$ to $\hat{P}$. Comparing Fig. 3.3(a) to Fig. 3.3(b), the dotted lines for RLA are generally shorter than those for CA.

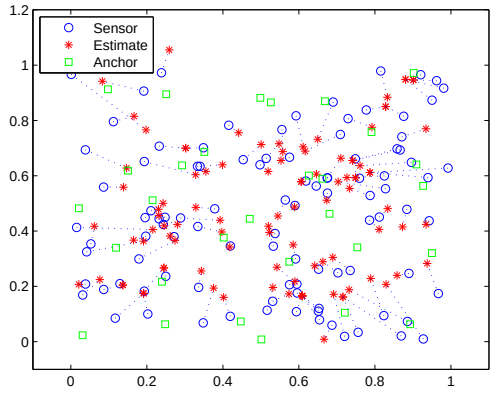


(a) Localization error of RLA (DOI=0.1, error = 0.1929)

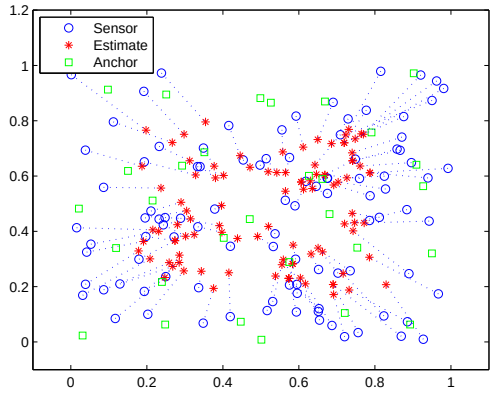


(b) Localization error of CA (DOI=0.1, error = 0.2872)

FIGURE 3.3: Location error with different transmission ranges

## 3.4 Summary

Range-free localization, while not as accurate as range-based, has the principal advantage of simplicity, i.e., there is no requirement for special hardware to measure time-of-arrival or time-difference-of-arrival. This is important for WSN in which sensors are low cost units, and in some applications where knowing accurate sensor positions is not critical. While determining $\hat{P}$ from CA is simple, it is possible to improve on its accuracy with some additional computations. The RLA provides such an option and the simulation results in Section 3.3 show that there is approximately a 2 to 30% gain in accuracy, depending on whether or not the anchors have identical ranges, and on the value of DOI.

# Chapter 4

# Mobile Element Assisted Cooperative Localization for Wireless Sensor Networks with Obstacles

When the sensor network is deployed in some special areas, the people cannot move in this area. If some anchors are dead, we need to use one mobile anchor, such as a robot, to cooperate with static sensors in the area. We study the localization algorithm in this scenario. In this chapter, we propose a multi-power-level mobile anchor assisted range-free algorithm for mobile anchor assisted WSNs with obstacles, in which the node localization problem is formulated as a convex optimization problem. By using a relay node, our scheme can effectively reduce the effects of obstacles on node localization. Furthermore, our scheme can calculate the positions of infeasible points caused by a complex radio transmission environment, which is recognized as a problem when the feasible set for localization inequalities is empty. Based on the derived localization error bound, an optimal movement scheduling method is proposed to reduce the total moving distance of the mobile element (ME) while assuring high localization performance, which can efficiently extend the lifetime of the ME.

## 4.1 Collaborative Localization using Mobile Element

In this section, we propose a collaborative node localization approach using an ME. We first introduce the technical preliminaries of our algorithm in subsection 4.1.1 and then formulate the localization problem as an optimization problem in subsection 4.1.2. We propose an algorithm for decreasing the impact of obstacles in subsection 4.1.3 and the movement scheduling algorithm for the MEs in subsection 4.1.4.

### 4.1.1 Background

In WSNs, a node can determine whether it is in the transmission radius of an anchor node according to the beacon signal received from the one-hop anchor. The anchor node can adjust its transmission radius by tuning the transmission power. For example, the TelosB mote is equipped with an IEEE 802.15.4 compliant Chipcon CC2420 radio, which has 31 transmission power levels between -25 and 0 dBm.

We assume an anchor node has $M$ levels of transmission power, and the corresponding transmission radii are $R_i$, $i = 1, 2, \ldots, M$. Normally, the ME is assumed to have a global positioning system (GPS) receiver and knows its position [58] [29]. During the moving period, the ME transmits beacon signals at varying power levels consecutively including its ID, current position, transmission power and transmission radius. After receiving these beacon signals, an unknown-position sensor can construct an effective constraint on its position.

For example, we assume that the current position for the ME is $a$ and its transmission radius is $R$. If the unknown-position sensor, at position $x$, receives the beacon signal, we can conclude that the distance between the two nodes satisfies

$$\|x - a\| \leq R. \tag{4.1}$$

Otherwise,

$$\|x - a\| > R. \tag{4.2}$$

Using the multiple transmission radius of the ME by tuning the transmission power at each position, the unknown-position sensor can obtain a set of inequalities on $x$:

$$r_i < \|x - a_i\| \leq R_i, \ i = 1, 2, ..., n \tag{4.3}$$

where $a_i$ is the position of the ME at the time $i$, $r_i$ (it might be zero) and $R_i$ are *valid radii* for that time. Herein, the valid constraint radii denote the corresponding lower and upper bounds, for the tightest constraint among all of the constraints that are constructed by all of the transmission powers for the mobile anchor node at position $a_i$.

Hence, the localization problem based on an ME with multiple transmission radius can be converted into the problem of solving a set of quadratic inequalities (4.3). Some algorithms (e.g., [52] [59]) are also based on the solution of a set of quadratic inequalities. However, their methods all assume that the set of quadratic inequalities (4.3) must have solutions. But, because of the complex transmission environment, there are two different location scenarios: the set of quadratic inequalities has a solution (i.e., the feasible set is nonempty); and the set of quadratic

inequalities have no solution (i.e., the feasible set is empty). For these two different scenarios, we propose a novel localization algorithm based on convex optimization to solve the problem whether the feasible set is empty or not. To the best of our knowledge, our proposed method is the only range-free algorithm using convex optimization to solve the problem when the feasible set is empty.

Note that the communications between wireless terminals are affected by several phenomena in practice, such as signal path loss, channel fading and shadowing [25]. The transmission radius and the location accuracy are affected by such phenomena. However, it is very difficult to quantify these effects as these practical factors are often unknown and complicated. Thus, in this work, we assume deterministic transmission radii, i.e., two wireless terminals cannot communicate if they are farther apart than the transmission radius. We note that such a deterministic model has been widely adopted in previous work on localization in WSNs, e.g. [52] [46] [59], and it is a reasonable approximation to the real communication behavior. Specifically, we use a numerical example to illustrate the impacts. We use the link model in [64] with the settings of the MICA2 mote to compute the packet reception ratio (PRR) between two sensors. The link model in [64] accounts for signal path loss and channel fading. Fig. 4.1 plots the PRR versus the distance between the two sensors under various transmission powers. Denote by $P_{Tx}$ the transmission power of the ME. When $P_{Tx} = 0\,\text{dBm}$, we set the transmission radius to be $R_{0\,\text{dBm}} = 9\,\text{m}$. When $P_{Tx} = 15\,\text{dBm}$, we set the transmission radius to be $R_{15\,\text{dBm}} = 18\,\text{m}$. We note that the ME is more powerful than the deployed low-cost motes and hence the transmission power of the ME can be much larger than that of the low-cost motes. We now compute the probability that a mote located in the ring region from $R_{0\,\text{dBm}}$ to $R_{15\,\text{dBm}}$ centered at the ME is successfully localized in the ring region. We note that a mote is localized in the ring region if it *cannot* hear the beacon packet when $P_{Tx} = 0\,\text{dBm}$ and it *can* hear the beacon packet when $P_{Tx}$ increases to 15 dBm. From Fig. 4.1, the average probabilities that a mote located in the ring region *cannot* and *can* hear beacon packet when $P_{Tx} = 0\,\text{dBm}$ and $P_{Tx} = 15\,\text{dBm}$ are 0.936 and 0.888, respectively. Therefore, the average probability that a mote located in the ring is successfully localized in the region is $0.936 \times 0.888 = 0.831$. We note that we can improve this success probability by adopting a larger transmission power interval, e.g., we can use 0 dBm and 20 dBm. However, doing so will introduce larger range estimation error, i.e., $e$ given by (4.11) below. In practice, we can balance such a trade-off to meet different requirements on localization performance.

### 4.1.2 Localization Algorithm using Convex Optimization

In real environments, the actual transmission radius varies in different directions of radio propagation because of the non-isotropic properties of the propagation medium and the heterogeneous properties of devices. According to the model of [19] to model this radio irregularity, all nodes

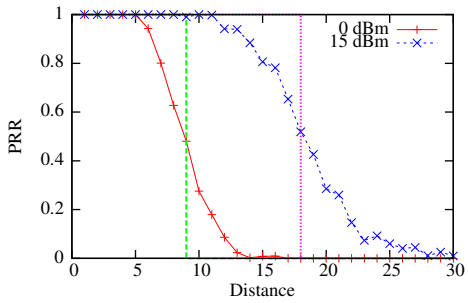


FIGURE 4.1: The packet reception ratio (PRR) vs. the distance between two MICA2 motes under various transmission powers.

within half of the maximum transmission radius of anchors are guaranteed to hear from the anchor. If nodes are beyond the maximum transmission radius, they cannot hear from the anchor. If nodes are between the maximum transmission radius and half of that radius, three scenarios are possible: (1) symmetric communication, (2) unidirectional asymmetric communication, and (3) no communication. Therefore, it is possible that there is no communication between two nodes although their relative distance is smaller than their ideal transmission radius. In this case, the inequalities for the original optimization problem will have no solutions and an infeasible case would occur.

In order to deal with the case with an empty feasible set, we propose a novel convex position estimation algorithm, which can provide good position estimation accuracy in both the feasible case and the infeasible case.

As shown in Fig. 4.2, for the single constraint case ($r < \|x - a\| < R$), it is easy to see that an efficient position estimate lies on the circle with center $a$ and radius $\frac{R+r}{2}$. In the figure, the square indicates the possible position for the optimal position estimate and the black dot denotes the anchor node with position $a$.

The position estimate can be found by minimizing the following expression:

$$(\|x - a\| - r)^2 + (\|x - a\| - R)^2.$$

Inspired by the single constraint case, for the inequalities under multiple constraints, we can seek an optimal position estimate by solving the following problem:

$$\min_x \sum_i \Big[(\|x - a_i\| - r_i)^2 + (\|x - a_i\| - R_i)^2\Big]. \tag{4.4}$$

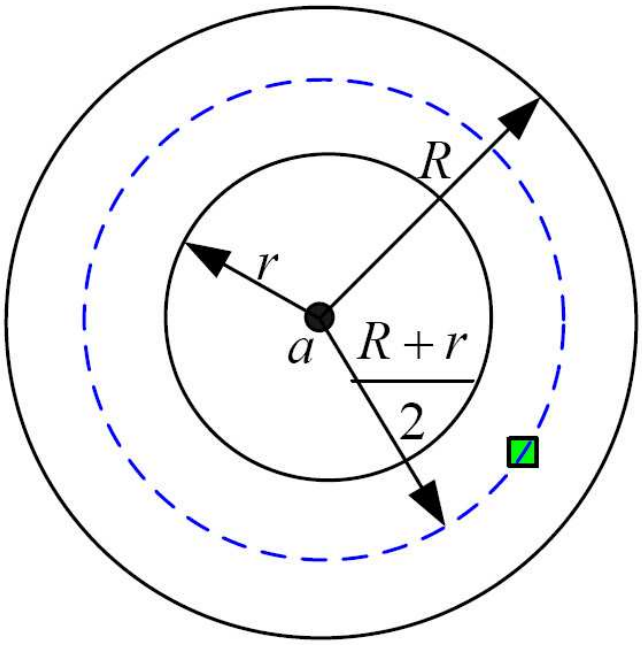


FIGURE 4.2: The single constraint case

Obviously, the problem (4.4) is nonconvex. Moreover, this problem cannot be directly approximated by using convex relaxation techniques like that of [3]. To approximately solve the problem via convex relaxation techniques, we transform it to the following problem[1]:

$$\min_{x} \sqrt{\sum_{i} \left[ (\|x - a_i\|^2 - r_i^2)^2 + (\|x - a_i\|^2 - R_i^2)^2 \right]}. \tag{4.5}$$

Although, the problem (4.5) is still nonconvex, we can turn it into a convex problem by using a convex relaxation technique. Firstly, we write the problem as follows:

$$\begin{aligned} &\min_{x,y} \sqrt{\sum_{i} \begin{bmatrix} (y - 2a_i^T x + \|a_i\|^2 - r_i^2)^2 \\ +(y - 2a_i^T x + \|a_i\|^2 - R_i^2)^2 \end{bmatrix}} \\ &s.t.\ \ y = \|x\|^2. \end{aligned} \tag{4.6}$$

Then by relaxing the equality constraint in (4.6) into an inequality constraint, we obtain the following convex problem:

$$\begin{aligned} &\min_{x,y} \sqrt{\sum_{i} \begin{bmatrix} (y - 2a_i^T x + \|a_i\|^2 - r_i^2)^2 \\ +(y - 2a_i^T x + \|a_i\|^2 - R_i^2)^2 \end{bmatrix}} \\ &s.t.\ \ \|x\|^2 \le y. \end{aligned} \tag{4.7}$$

[1]The possible case where there is only the lower bound $r_i$ or the upper bound $R_i$ is not considered in this formulation. However, such a case can still be handled by using the same convex relaxation technique.

Using epigraph form[6], we can further transform it into a standard linear cone programming problem:

$$\begin{aligned} \min_{x,y,v,t} \quad & t \\ \text{s.t. } & \|v\| \le t \\ & y - 2a_i^T x + \|a_i\|^2 - r_i^2 = v_{i1} \\ & y - 2a_i^T x + \|a_i\|^2 - R_i^2 = v_{i2} \quad \forall i \\ & \|x\|^2 \le y \end{aligned} \tag{4.8}$$

where $v = \begin{bmatrix} v_{11} & v_{12} & \cdots & v_{i1} & v_{i2} & \cdots & v_{n1} & v_{n2} \end{bmatrix}^T$. Herein, in order to write in the standard form, we introduce a dummy variable $t$. $t$ is also introduced in the epigraph model of the problem; please refer to [6]. All vector variables in this paper are column vector. The resulting problem can be solved by using efficient interior-point algorithms, e.g., the solver SeDuMi[50].

### 4.1.3 Algorithm for Decreasing the Impact of Obstacles

In this paper, we assume that boundary nodes around the obstacle have been discovered by some boundary recognition algorithms [16], so that each sensor node knows whether it is a boundary node or not. Only boundary nodes can participate in contention for relaying beacons from the ME because their rebroadcasts may cover some blind areas as shown in Fig. 4.3. Hearing a beacon from the ME, boundary nodes will compete to relay this location information through a distributed contention process. The probability that a candidate node wins the contention depends on the node's remaining energy and the number of neighboring sensors. The node with greater remaining energy and greater number of neighbors has higher priority to be the optimal relay node. The proposed selection scheme for the optimal relay node is concluded as follows: Receiving a beacon from the ME, a boundary node sets a backoff timer which defines the amount of time that the node must wait before rebroadcasting the location information. The backoff time $\delta$ is calculated as

$$\begin{aligned} \delta = (\alpha(used\_energy/initial\_energy) + \\ \beta/num\_neighbors) * max\_delay \end{aligned} \tag{4.9}$$

where $\alpha$ and $\beta$ are the modification coefficients to provide different weights for different parameters. We can see that a greater remaining energy and a greater number of neighbors will lead to a shorter backoff time. If a candidate boundary node does not hear any beacon signal from other sensors during its backoff time, it will rebroadcast the beacon signal and other boundary nodes will cancel their contentions if they receive the rebroadcast of the beacon. As a result, the node with the highest priority will rebroadcast first and win the competition to serve as the relay for

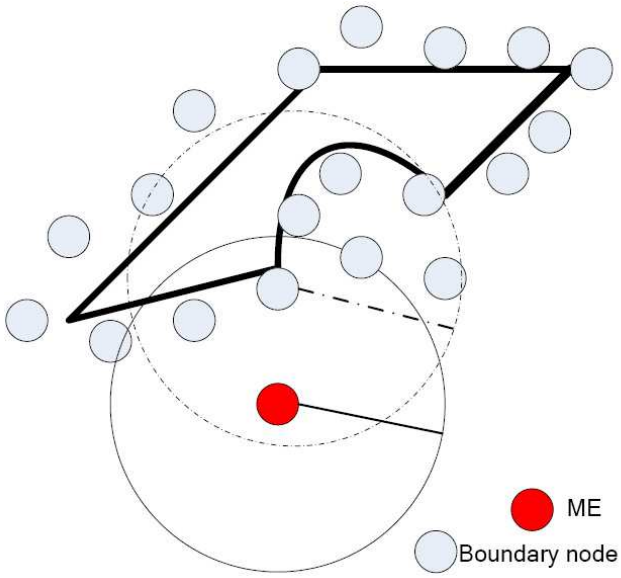


FIGURE 4.3: A sensor network with an obstacle

the ME's beacon signal. Note that this distributed relay node selection process is triggered by the reception of a beacon message from the ME. Therefore, we do not require an explicit time synchronization protocol among the candidate relays. They are implicitly synchronized by the beacon message. However, due to the existence of propagation delay and receive-to-transmit switch time, the relay selection may fail when one relay cannot hear the best relay's rebroadcast of the beacon message. This is the case when the backoff timer of a candidate relay expires before the rebroadcast of the best relay arrives at it. However, such a case is rare according to the analysis in [5]. For example, selecting $c/\lambda = 1/200$ will result in a collision probability less than 0.6% where $c$ is the propagation delay and switching time and $\lambda$ is the max delay in equation (4.9). Typically $c = 5\mu s$, this means the max delay can be 1 ms, which implies the best relay will be selected within 1 ms. In this way, we can deliver the ME's location information to some areas that cannot receive the ME's direct communication. Similarly to (4.3), the unknown-position sensor in these special areas can obtain a set of inequality constraints on $x$ :

$$\left|R_i - R_{relay}\right| \leqslant \|x - a_i\| \leqslant R_i + R_{relay}, \quad i = 1, 2, \ldots, n \tag{4.10}$$

where $R_{relay}$ is the current transmission radius for the relay node and $\left|R_i - R_{relay}\right|$ is absolute value. We can also use the proposed convex localization algorithm to solve the problem (4.10). Based on this scheme, we can efficiently decrease the impact of the obstacle on node localization and improve the location accuracy.

Note that the beacon signal transmission is affected by several affecting phenomena such as signal path loss and channel fading. It is difficult to solve this problem well in WSNs due to its hardware constraints. The sensors that cannot be covered directly by the ME due to physical obstacles will have larger localization errors than the requirement since (4.10) gives a looser

bound than (4.3). Due to fading and shadowing of wireless channels, it is possible that the relay node cannot successfully relay the beacon signal to the unknown-position sensor within the area that cannot receive the ME's direct communication. However, the ME will transmit beacon signals at varying power levels consecutively when it is stationary. With different beacon signals at a given position of ME, the selected relay node will differ. Thus it will increase the probability of covering the unknown-position sensor within the area that cannot receive the ME's direct communication. In the worst case, if the relay node still cannot cover it, we will consider it as a blind node that cannot be localized.

### 4.1.4 Movement Scheduling for Mobile Elements

Several types of MEs capable of free movement are currently available, e.g., Packbot [45] and Robomote [14]. In practice, the ME cannot visit some positions due to physical obstacles. We assume that the regions that the ME cannot visit are known. We only consider the minimal set of hexagons that cover the visitable region. Due to power constraints, the ME is capable of only low-speed and short-distance movement in practical deployments. For instance, the normal speed of several mobile sensor platforms (e.g., Packbot and XYZ) is only $0.5 \sim 2m/s$. An XYZ mobile sensor node that is powered by two AA batteries can move only about 165 meters before exhausting its power. Therefore, the movement trace of the ME must be efficiently planned in order to maximize the number of localized unknown-position sensors with the required localization accuracy.

The optimal movement schedule for MEs in our algorithm needs to achieve the shortest path length so that the ME covers the entire area with the shortest time and consumes the minimum energy. Based on the derived localization error bound (which will be derived in Section 4.2), we propose an optimal movement schedule for MEs as follows:

When the ME has no prior information about sensors' positions, in order to guarantee that each sensor is localized with error $\epsilon$, the entire geographical region should be covered by disks with radii $r_d$ centered at the beacon points of the ME. The most efficient coverage is the hexagonal tiling of the entire region, in which the edge length of each hexagon is $r_d$ and each beacon point is at the center of each hexagon. In the optimal movement schedule of the ME, the center of a hexagon is visited by the ME once. Obviously, the shortest length of a path that crosses a hexagon is $\sqrt{3}r_d$. In the line-by-line scan as shown in Fig. 4.4, the shortest path length is achieved. Therefore, the line-by-line scan is an optimal movement schedule of the ME.

When each sensor has coarse prior information about its position, the ME does not need to cover the entire region. Suppose there are $N$ sensors and sensor $i$ is in region $A_i$ with high probability. Let $\{H_i\}$ denote the minimal set of hexagons that covers the united regions $\bigcup_{i=1}^{N} A_i$, where $H_i$ is one of the hexagons in the hexagonal tilings of the entire geographical region. Note that $\{H_i\}$

**Algorithm 1** Find the shortest Hamiltonian path

**Input:** $G = (V, E)$, starting point $v_0$
**Output:** The shortest Hamiltonian path in $G$

```
cost = INT_MAX
for v ∈ V\v_0 do
  creat edge e that connects v_0 and v with cost of -INT_MAX
  E' = E ⋃ e, G' = (V, E')
  P = TSPsolver(G')
  if |P\e| < cost then
    hpath = P\e
    cost = |P\e|
  end if
end for
return hpath
```

can be found by checking whether each hexagon has intersection with $\bigcup_{i=1}^{N} A_i$, and hence in polynomial time. Construct a undirectional graph $G = (V, E)$, where $V$ is the set of centers of $\{H_i\}$ and $E$ is the set of Euclidean distances between any two points in $V$. The movement schedule of the ME can be formulated as the shortest Hamiltonian path problem. Specifically, given a starting point that is a vertex in $V$, find the shortest path that visits each vertex in $V$ exactly once. We note that the problem of finding a Hamiltonian path is NP-complete and therefore the problem of finding the shortest Hamiltonian path is also NP-complete [17].

We now propose a heuristic algorithm to solve the movement scheduling problem formulated above by using any solver of the travelling salesman problem (TSP). Note that the optimal solution to the TSP is the shortest Hamiltonian cycle for the given graph $G$. Our basic idea is as follows. We first connect a vertex $v$ and the starting point with an edge of large negative cost, and then apply the TSP solver to the modified graph. Heuristically, this added edge will be included in the TSP solution and the shorest Hamiltonian path that ends at $v_i$ can be found by removing the added edge from the TSP solution. By iterating $v \in V$, we can find the shortest Hamiltonian path. Algorithm 1 shows the pesudo code of the heuristic algorithm. In the pesudo code, `INT_MAX` represents the maximum integer of the programming language, and $|P\backslash e|$ represents the cumulative cost of the path $P\backslash e$.

## 4.2 Performance Analysis

### 4.2.1 Localization Error Bounds

Wang *et al.* [57] investigated the network coverage for range-based target localization applications. We compare our method with their method implemented in the ideal environment without obstacles. As the simulation results shown in subsection 4.3.3, our algorithm outperforms their method. Hence, based on their analytical localization error bound, it is feasible to extend their

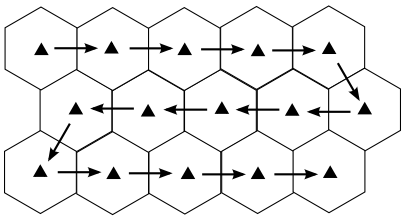

FIGURE 4.4: The optimal movement schedule of the mobile anchor when no information about sensors' positions is available. The triangles represent the way points of the mobile anchor. The edge length of each hexagon is $r_d$.

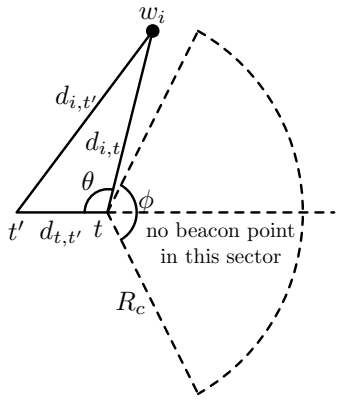


FIGURE 4.5: The ME cannot distinguish two points $t$ and $t'$.

analysis to the scenario of range-free localization using an ME and thereby to derive a loose localization error bound for our localization algorithm. In [57], Wang *et al.* proved a sufficient condition for achieving a target localization error of $\frac{4\sqrt{3}e}{3}$, where $e$ is the maximal range estimation error. The major limitation of their result is that they consider only a specific value of localization error. In this section, we will extend their result to the scenario of range-free localization using ME with *any* required localization error.

We first derive the maximal range estimation error, *i.e.*, $e$, under the scenario of range-free localization.

Let $R_i$ denote the transmission radius when the ME broadcast beacon using the $i^{\text{th}}$ transmission power level. We assume $R_i < R_j$ if $i < j$. The ME can determine the distance from a sensor, denoted by $d$, which satisfies $R_i \leq d \leq R_{i+1}$. The optimal estimate of the sensor position lies on the circle centered at the ME and with radius $\frac{R_i+R_{i+1}}{2}$. Hence, the distance estimate made by the ME is $\frac{R_i+R_{i+1}}{2}$ and the maximal range estimation error is given by

$$e = \max_i \left\{ \frac{R_{i+1} - R_i}{2} \right\}. \tag{4.11}$$

In [57], the network resolution is defined to facilitate derivation of the localization error bound. We now extend this definition to the scenario of range-free localization using an ME.

*Definition 1:* Two points $t$ and $t'$ are *distinguishable* if the ME can always distinguish whether a sensor is at point $t$ or $t'$ through the measurements provided by the ME at different locations. The *network resolution* is the minimal distance $l$, such that the ME can distinguish any pair of points when the distance between them is larger than $l$.

The following lemma gives the relationship between network resolution and the localization error bound, which has been proved in [57]. We refer interested readers to [57] for the details of the proof. We note that it also holds for the scenario of range-free localization using ME.

*Lemma 1 [57]:* If the network resolution is better than $\sqrt{3}\epsilon$, the localization error is upper bounded by $\epsilon$.

The following theorem gives a sufficient condition for achieving a localization error of $\epsilon$, which enables us to schedule the movement of ME to satisfy the required localization error.

*Theorem 1:* The localization error is upper bounded by $\epsilon$ if there is at least one ME beacon point in any arbitrary sector of radius $R_c$ and angle $\phi$, where $R_c$ is the maximal transmission radius of the ME, $\phi$ is given by

$$\phi = 2\arccos\left(\frac{2e}{\sqrt{3}\epsilon}\right), \tag{4.12}$$

and $\epsilon > \frac{2}{\sqrt{3}}e$. Note that $e$ is the maximal distance estimation error of the ME when the sensor is within $R_c$ meters from the ME, which is given by (4.11).

*Proof:* From Lemma 1, a sufficient condition for the localization error of $\epsilon$ is that the network resolution provided by the ME is $\sqrt{3}\epsilon$. We prove this theorem by contradiction. Suppose the network resolution is worse than $\sqrt{3}\epsilon$, i.e., we can find at least one pair of points $t$ and $t'$ which are apart by more than $\sqrt{3}\epsilon$, and the ME cannot distinguish them. Now we will prove that if the conditions for this theorem are satisfied, such a network resolution cannot be true and hence the localization error of $\epsilon$ is guaranteed.

Suppose two points, $t$ and $t'$, cannot be distinguished by the ME and the distance between them is $d_{t,t'} \geq \sqrt{3}\epsilon$. We denote the sector of radius $R_c$ and angle $\phi$ by $(R_c, \phi)$. As we assumed that there is at least one ME beacon point in any sector of $(R_c, \phi)$, there must be at least one beacon point within $R_c$ meters from $t$. Suppose this beacon point is $w_i$ as shown in Fig. 4.5. A necessary condition for $t$ and $t'$ to be indistinguishable is

$$|d_{i,t} - d_{i,t'}| \leq 2e; \tag{4.13}$$

otherwise, $t$ and $t'$ can be distinguished by the ME at beacon point $w_i$. Moreover, $t'$ must be within $R_c$ meters from $w_i$, as otherwise $t$ and $t'$ can be distinguished by the ME. Without loss of generality, we assume $d_{i,t} \leq d_{i,t'}$ and therefore $d_{i,t'} \leq d_{i,t} + 2e$ according to the above necessary

condition. As shown in Fig. 4.5, according to the law of cosines, we have

$$\cos\theta = \frac{d_{i,t}^2 + d_{t,t'}^2 - d_{i,t'}^2}{2d_{i,t}d_{t,t'}} \tag{4.14}$$

$$\geq \frac{d_{i,t}^2 + d_{t,t'}^2 - (d_{i,t} + 2e)^2}{2d_{i,t}d_{t,t'}} \tag{4.15}$$

$$= \frac{d_{t,t'}^2 - 4e^2 - 4d_{i,t}e}{2d_{i,t}d_{t,t'}}. \tag{4.16}$$

As $d_{t,t'} \geq \sqrt{3}\epsilon > 2e$, we have $d_{t,t'}^2 - 4e^2 > 0$. Therefore,

$$\cos\theta > -\frac{2e}{d_{t,t'}} \geq -\frac{2e}{\sqrt{3}\epsilon}. \tag{4.17}$$

Accordingly,

$$0 \leq \theta < \arccos\left(-\frac{2e}{\sqrt{3}\epsilon}\right) = \pi - \arccos\left(\frac{2e}{\sqrt{3}\epsilon}\right) \tag{4.18}$$

and

$$\phi < 2(\pi - \theta) \leq 2\pi. \tag{4.19}$$

There is no beacon point within the sector of $(R_c, 2(\pi - \theta))$ centered at $t$ and bisected by ray $t't$, otherwise, $t$ and $t'$ can be distinguished. However, as $2(\pi - \theta) > \phi$, this result is a contradiction to the assumption that there is at least one beacon point in any sector $(R_c, \phi)$.

From Theorem 1, when $\epsilon \in \left(\frac{2}{\sqrt{3}}e, \infty\right)$, $\phi \in (0, \pi)$. Theorem 1 can be extended to the disk coverage model as follows.

*Corollary 1:* The localization error is upper bounded by $\epsilon$ if disks of radius $\frac{\sin\frac{\phi}{2}}{1+\sin\frac{\phi}{2}}R_c$ centered at the ME's beacon points cover the entire field, where $R_c$ is the maximal transmission radius of the ME and $\phi$ is given by (4.12).

Proof: A sector of $(R, \phi)$ contains an inscribed circle of radius $r_d = \frac{\sin\frac{\phi}{2}}{1+\sin\frac{\phi}{2}}R_c$. Therefore, if the disks of radius $r_d$ centered at the ME's beacon points cover the entire field, there will be no sector $(R_c, \phi)$ which contains no sensor and hence the location estimation error bound is guaranteed according to Theorem 1.

We note that the disc coverage model has several advantages over the sector coverage model. First, the disc coverage problem has been extensively studied in the previous literature [7]. The previous results and algorithms can be applied to schedule the movement of the ME. Second, the disc model is easier than the sector model in the geometric treatment due to its simplicity. Therefore, we adopt the disc coverage model to schedule the movement of ME in this paper.

### 4.2.2 Communication Cost and Power Consumption

The number of messages that a sensor node needs to transmit is treated as the communication cost in our localization algorithm. In our localization process, the MEs will perform the broadcasting operation at every time slot. Thus the communication cost is related to the number of beacon signals, which can be calculated as follows:

For the communication cost in the line-by-line case, on letting $l$ be the width of the deployment area, the number of hexagonal tilings in a row can be calculated as $l/\sqrt{3}r_d$. In the same way, on letting $h$ be the height of the deployment area, the number of rows is $h/\sqrt{3}r_d$. For each hexagonal tiling, we assume the ME will beacon twice. Therefore, the total number of beacons is $2hl/3r_d^2$. For the communication cost in the TSP case, the number of beacon points is $2\{H_i\}$, i.e., two times the size of the set $\{H_i\}$. Thus, it is upper bounded by the communication cost of the line-by-line case. The ME broadcasts to unknown-position sensors a hello message with its ID, location and some recognize-bits which amounts to only several bytes. For low beacon point density, this would require roughly hundreds of bytes.

We can evaluate the corresponding energy consumptions of our approach. We account for the energy consumed in locomotion of the ME, wireless communication, and idle state at local sensors. We assume that the ME is a wheeled robot such as the Robomote [14]. The energy consumed in locomotion by a wheeled robot, denoted by $E_M(d)$, can be approximated by $E_M(d) = k \cdot d$ [56], where $d$ is the moving distance and $k = 2\,\mathrm{J/m}$ if the ME moves at optimal speed. For typical low-power transceivers such as CC2420, the energy consumed in wireless communication, denoted by $E_C(d)$, can be modeled as $E_C(d) = m \cdot (a + b \cdot d^2)$ [38], where $d$ is the transmission distance, $m$ is the number of bits transmitted, and $a$ and $b$ are constants. $a$ and $b$ can be set to be $0.6 \times 10^{-7}\,\mathrm{J/bit}$ and $4 \times 10^{-10}\,\mathrm{J/m^2 \cdot bit}$ according to the experiments in [38]. The power consumption of an idle node is set to be 21 mW, which is consistent with that of the TelosB mote [1]. We assume that a node stays asleep when it is outside of the communication range of the ME during the localization phase. Moreover, we ignore the power consumption of a sleep node, as it is much less than the idle state power consumption. For instance, a TelosB mote consumes $1\,\mu\mathrm{W}$ in sleep mode [1].

In our line-by-line case, the energy consumed in wireless communication by the ME is $E_c(R_i) = m\cdot(a+b\cdot R_i^2)\cdot\frac{2hl}{3r_d^2}(J)$, the energy consumed in locomotion by the ME is $E_m(d) = 2\left(\frac{hl}{\sqrt{3}r_d} - \sqrt{3}r_d\right)(J)$, and the average power consumption of sensors in the ME radio coverage area is $E_s = 21 \cdot N_s(mW)$, where $N_s$ is the average number of sensors in the ME radio coverage. Therefore, $N_s = \rho \cdot \pi R_i^2 = \frac{N\pi R_i^2}{A}$, where $N$ is the total number of sensors and $A$ is the total area of the network.

For the method of [59], if it adopts the dense-straight-line (DSL) movement pattern and the broadcasting interval of the beacon is 0.25 meters, the energy consumed in wireless communication of their method is $E_c = m \cdot (a + b \cdot R_i^2)(\frac{hl}{4R_i^2} + \frac{h}{2R_i}) \cdot 4(J)$, the energy consumed in locomotion by the mobile beacon is $E_m = 2\left[(l + 2R_i) \cdot (\frac{h}{2R_i} + 1) + h\right](J)$, and the power consumption of sensors in the ME radio coverage area is $E_s = 21 \cdot N_s(mW)$.

By setting $\phi = \frac{2\pi}{3}$ and $R_i = 45\ m$, we have the following conclusion. The energy consumed in wireless communication by the ME in our approach is slightly smaller than that of the method in [59]. However, the energy consumed in locomotion of the ME in our method is significantly smaller than that of the method in [59]. The power consumption of idle sensors is almost the same for both methods.

## 4.3 Numerical Results

In this section, simulation results are presented and analyzed. We consider a 2-dimensional region with a size of 100 m x 100 m. We assume the ME has two level transmission power with the transmission radii $r$ and $R = 2r$, respectively. First, we deploy 100 sensor nodes randomly and the transmission radius $r$ is set to 15 meters. All simulation results are averaged over 100 network scenarios. The average localization error is used to evaluate the performance for our localization algorithm. The average localization error is defined as follows:

$$error = \frac{1}{N} \sum_{i=1}^{N} \|x_i - \hat{x}_i\| \times \frac{1}{r}, \tag{4.20}$$

where $x_i$ is the real position for node $i$, $r$ is the maximum transmission radius and $\hat{x}_i$ is the estimated position of node $i$. Note that we normalize the absolute localization error using maximum transmission radius. For instance, the error 20% means that the real localization error is 20% of maximum transmission radius.

### 4.3.1 Performance in the Ideal Environment

In this subsection, we give the simulation results for different algorithms in the ideal situation, namely, there is no obstacle in the sensing area. We use the degree of irregularity (DOI) to indicate the radio irregularity characteristic. Its value denotes the maximum range variation per unit degree change in the direction of radio propagation. Fig.4.6(a) and 4.6(b) show the simulation results in this ideal situation, where the true nodes are denoted by circles, the position estimates are denoted by asterisks, and the lines that link the true nodes and the estimates represent the estimation errors. It is clear from Fig.4.6(a) and 4.6(b) that our algorithm works better than the algorithm of [59] in terms of the average localization error.

In practical environments, the actual transmission radius varies in different directions of radio propagation because of the non-isotropic properties of the propagation medium and the heterogeneous properties of devices. In this experiment, we investigate the impact of irregular radio patterns on the precision of our proposed localization algorithm. similar to [59], we use a random value to denote the variance of path loss, and this random value follows a Weibull distribution. Parameter DOI determines the maximum variance. Using this DOI model, we not only obtain the property that the variance of path loss is distinct in every direction but also show that pass losses in the same direction may be varying due to the dynamic changing of environment. As shown in Fig.4.7(a), the localization accuracy of our algorithm decreases as the DOI increases. When the DOI is smaller than 0.1, the localization error varies slightly. Fig.4.7(a) indicates that our method outperforms the method of [59] in terms of the average localization error with the various values of DOI. We evaluate the localization accuracy of our localization algorithm in both the proposed and random movement strategy with the different DOI. Fig.4.7(b) indicates that our localization algorithm using the proposed movement strategy outperforms than that using the random movement strategy.

### 4.3.2 Performance in the Non-ideal Environment

For the next set of experiments, we use channel fading model to indicate the effect of obstacle on localization accuracy. Herein, we use a fading coefficient *(f)* that represents the percentage of total mobile beacon points that cannot be heard by the sensor at any given time. This models obstacles encountered in the sensing area that limit the number of mobile beacon points that can be heard at any point. As Fig.4.8(a) and 4.8(b) illustrate, our algorithm outperforms the algorithm of [59] in terms of the average localization error in this non-ideal environment.

### 4.3.3 Performance Comparison with a Range-based Method

In this section, we employ the range-based localization algorithm in [57] as the baseline. Fig.4.9(a) and 4.9(b) show the localization results by our method and the baseline algorithm, respectively, in the ideal environment without an obstacle. We can see from these two figures that our method outperforms the baseline algorithm in terms of average localization error. Specifically, the average localization errors are 12.03% and 18.68%, respectively. Note that the settings of our method can be configured to meet any required localization error as discussed in section 4.2.1. However, the baseline algorithm can only achieve a specific localization error that depends on the range estimation error of the ME. Therefore, our method outperforms the baseline method.

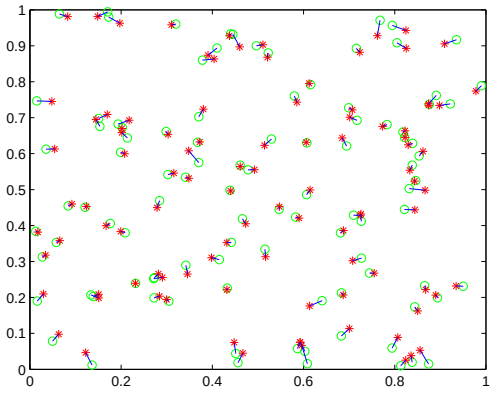


(a)

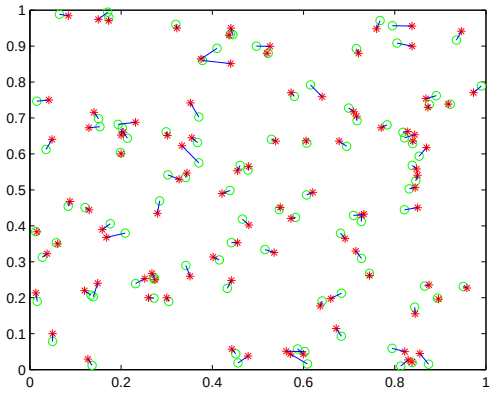


(b)

FIGURE 4.6: Performance comparison: (a) Localization error of our method (DOI=0.2, error = 11.68%); (b) Localization error of method [59] (DOI=0.2, error = 13.7%)

## 4.4 Summary

We have presented a new cooperative localization scheme that can achieve high localization accuracy in mobility-assisted wireless sensor networks when obstacles exist. Considering the complex localization scenario, namely, the feasible set is empty, a convex localization algorithm has been presented to address the effects of non-ideal transmission of radio signals. We have developed an optimal movement schedule for MEs that can achieve a shortest path under expected localization accuracy. It has been shown in the simulation results that the proposed cooperative localization scheme can achieve high localization accuracy by including a mobile element. In future work, we intend to verify and improve the proposed cooperative localization scheme using real sensors in a mobility-assisted wireless sensor networks. We will extend our work to address other limited mobility models of MEs, such as the straight-line mobility model of the XYZ mobile sensor [32]. Using distributed space-time-codes [5] to reduce the impact of channel fading on the cooperative localization algorithm is also an important issue to be considered

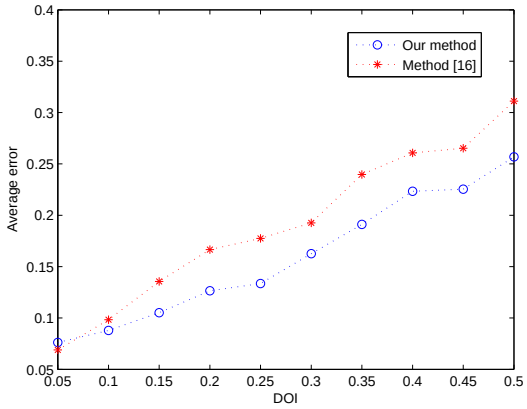


(a)

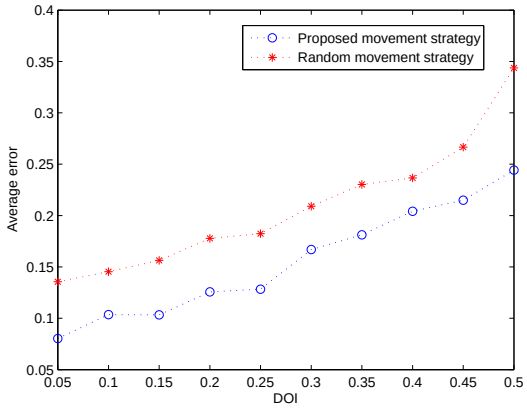


(b)

FIGURE 4.7: Performance comparison: (a) The average localization error vs. DOI; (b) Impact of movement strategy

in the future.

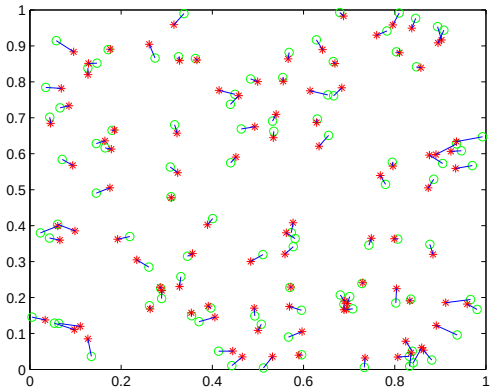


(a)

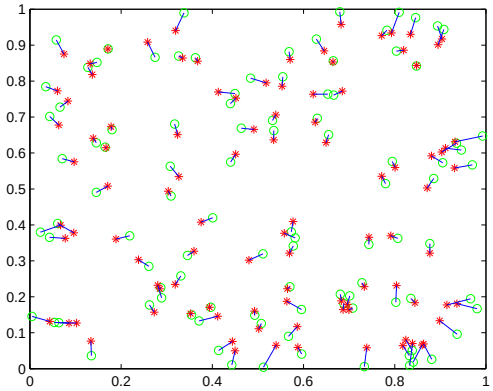


(b)

FIGURE 4.8: Performance comparison in the non-ideal environment: (a) Localization error of our method (DOI=0.25, $f$=0.1, error = 17.07%); (b) Localization error of method [59] (DOI=0.25, $f$=0.1, error = 19.34%)

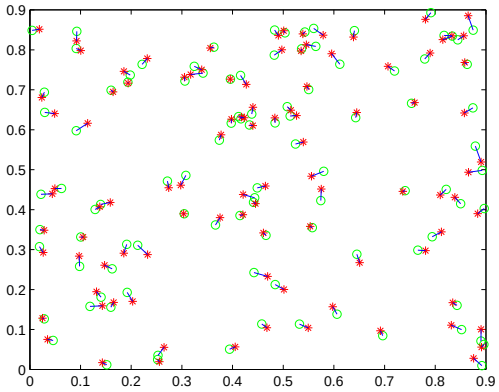


(a)

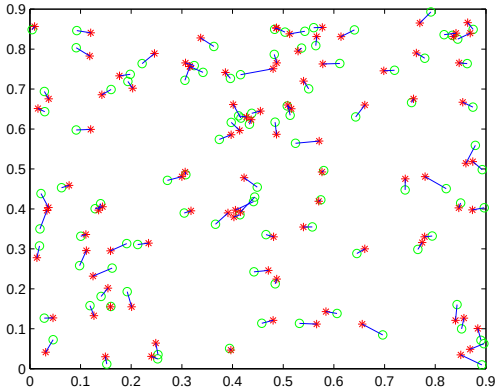


(b)

FIGURE 4.9: Performance comparison with a range-based method: (a) Localization error of our method (DOI=0.25, error = 12.03%); (b) Localization error of method [59] (DOI=0.25, error = 18.68%)

# Chapter 5

# Accurate and Efficient Node Localization for Mobile Sensor Networks

In Chapter 4, we include only one mobile anchor. In some scenario, all anchors and sensors are moving, such as mobile sensor networks. In this case, the movement trace may more complicated than we studied in the Chapter 4. The localization problem for mobile sensor networks is also very interest and important. In this chapter, we propose a range-free cooperative localization algorithm for mobile sensor networks by combining hop distance measurements and particle filtering. In the hop distance measurement step, a differential error correction scheme is devised to reduce the positioning error accumulated over multiple hops. A backoff-based broadcast mechanism is also introduced in our localization algorithm. It efficiently suppresses redundant broadcasts and reduces message overhead. The proposed localization method has fast converges with small location estimation error. We verify our algorithm in various scenarios and compare it with conventional localization methods. Simulation results show that our proposal is superior to the state-of-the-art localization algorithms for mobile sensor networks.

## 5.1 Algorithm Development

In this section, we provide the details of our proposed hop distance measurement and particle filter-based cooperative localization algorithm for mobile WSNs. For simplification purposes, we present our algorithm for the two-dimensional scenario. Intuitively, our work can be easily extended to the three-dimensional case. Our proposal can be divided into two main steps:

### 5.1.1 Hop Distance Estimation and Backoff-based Message Broadcast

In the first step, each anchor node broadcasts a beacon message throughout the network. The beacon message contains the anchor's location and a hop count with an initial value of zero. Each receiving node maintains the minimum hop count value per anchor node from all beacon messages it receives. Beacon messages with a higher hop count value from a given anchor node are ignored and discarded. On the other hand, valid beacon messages are forwarded with an incremented hop count after each hop. In this way, all nodes in the network can find their minimum hop counts to each anchor node. Nonetheless, this simple flooding method may result in excessive message overhead. To deal with this issue, we propose a backoff-based broadcasting mechanism described at the end of this section.

Conventional hop count localization methods require two separate flooding stages: (a) hop count accumulation and (b) average hop distance (*correction*). In comparison, our method combines the correction process with the hop count accumulation stage to reduce message transmissions. When the effective hop distance is calculated in the flooding process, the hop count is broadcasted simultaneously to all the nodes in the network. This approach effectively helps to reduce the number of transmitted messages, consequently reducing the network energy consumption and the time spent on computing a node's position.

Once an anchor node receives the hop count value from another anchor node, it estimates the average distance of one hop, namely *hop distance*, which will be used as a correction factor to be transmitted to the entire network. After receiving the hop distance, regular nodes multiply it by the hop count number to derive their estimated physical distances to the anchor nodes. For instance, the average hop distance between anchor nodes $i$ and $j$ is calculated as:

$$HopDistance_{i,j} = \frac{\sum_{i \neq j} \sqrt{(x_i - x_j)^2 + (y_i - y_j)^2)}}{\sum_{i \neq j} h_{i,j}} \tag{5.1}$$

where $(x_i, y_i)$ and $(x_j, y_j)$ are the coordinates of anchors $i$ and $j$, respectively, and $h_{i,j}$ is the number of hops between them. After hop distance estimation, it is straightforward to estimate the distance between two anchor nodes $i$ and $j$ as follows.

$$d_{est}^{i,j} = HopDistance_{i,j} \times h_{i,j}. \tag{5.2}$$

On the other hand, the actual distance, $d_{true}^{i,j}$, between anchor nodes $i$ and $j$ is given by

$$d_{true}^{i,j} = \sqrt{(x_i - x_j)^2 + (y_i - y_j)^2} \tag{5.3}$$

Following (5.2) and (5.3), the difference between the estimated and actual distances, denoted by $e^{i,j}$, can be expressed as

$$e^{i,j} = d^{i,j}_{est} - d^{i,j}_{true}, \tag{5.4}$$

which corresponds to the estimation error.

Here, we propose the usage of the differential error in (5.4) as a correction term to the original hop distance estimation presented in (5.1). The effective average hop distance, $EffHopDistance_{i,j}$, between anchor nodes $i$ and $j$ is defined as [12]:

$$EffHopDistance_{i,j} = HopDistance_{i,j} - \frac{e^{i,j} + e^{i,m}}{h_{i,j} + h_{i,m}}, \tag{5.5}$$

where $h_{i,m}$ is the number of hops in-between, and $m$ is the second-closest anchor node to the unknown-position node $k$.

When anchor nodes $i$ and $m$ broadcast their average hop distances from $j$ to regular node $k$, the related hop count value will also be broadcasted simultaneously to reduce the total number of transmitted messages. After obtaining both messages from $i$ and $m$, $k$ calculates $e^{i,j}$ and $e^{i,m}$ using eq. (5.4). Subsequently, the effective average hop distance can be calculated using the received beacon information via eq. (5.5). Based on eq. (5.5), $k$ can compute its distance $d^{k,j}_{eff}$ to anchor node $j$:

$$d^{k,j}_{eff} = EffHopDistance_{k,j} \times h_{k,j} \tag{5.6}$$

If $i$ is the closest anchor node to $k$, it is more accurate to estimate the distance between $k$ and $j$ by using $EffHopDistance_{i,j}$. From this principle, a generalization to any regular node is possible. That is, a given regular node can use the effective average hop distance obtained from its closest anchor node to calculate the distances to its neighbor nodes.

As shown in Fig. 5.1, simple flooding method suffers from high message overhead when used to provide location information to neighbor nodes, thus we propose a backoff-based broadcast mechanism to suppress redundant messages. A node may receive sequential beacon messages about the same anchor and each one of them leads to a smaller hop count. As a result, this node may need to forward it several times. Fig. 5.1 illustrates an anchor message propagation initiated by anchor node $A$. Due to the random exponential backoff of the MAC layer, node $C$ may broadcast $A$'s message before node $B$. Suppose that node $D$ wins the next channel contention, and both nodes $E$ and $F$ set their minimum hop count to 3. It is possible that node $B$ further fails the channel contention dispute with node $E$, and thus node $E$ broadcasts an anchor message containing the wrong minimum hop count information before it notices the right value. Once the order is altered, the error is accumulated from each broadcast. Node $E$ only needs to broadcast another anchor message after hearing the lower hop count information from node $B$, but nodes that are farther away from the anchor node may need to forward it several times to

correct the accumulated error. We observe that nodes at the border of the transmission range of

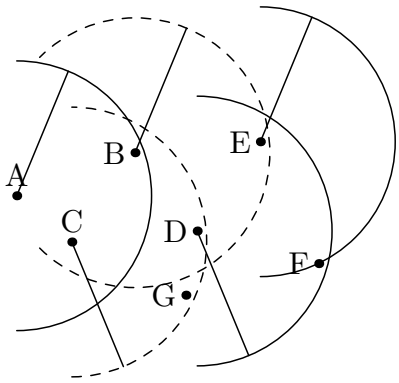


FIGURE 5.1: An example of anchor message propagation

a sender have the widest coverage of its two-hop neighbors. Therefore, we should give these nodes the highest priority to broadcast. This has been extensively studied to reduce redundant broadcasts and collisions [4, 20, 61]. However, previous methods only alleviate the redundancy problem rather than completely suppressing it.

Giving receivers farther away from a sender higher priority to broadcast could solve the redundancy mentioned above. However, node $G$ still suffers from redundant broadcast. Previous methods would allow node $B$ to broadcast before node $C$. According to these methods, node $E$ should broadcast before node $D$ and it is likely that node $E$ would also broadcast before node $C$. If node $F$ wins the following channel contention, node $G$ would get a wrong hop count of 3.

Based on these observations, we propose a backoff-based flooding which works as follows. Nodes that are far away from the sender are expected to have a weaker received signal strength. Therefore, we set $ISS = Pr - RXThresh$ for each node, where $ISS$ is the increase in signal strength, $Pr$ denotes the received signal power, and $RXThresh$ denotes the minimum signal power for successfully decoding a packet. Each node defers its broadcast of the anchor message for $ISS * unit\_delay$ time units, where $unit\_delay$ should be large enough to cope with the random backoff of the MAC layer. Otherwise, node $C$ may still broadcast before node $B$ due to its winning of contention in channel access.

Supposing that node $B$ is on the border of the transmission range of node $A$, it will broadcast immediately after hearing an anchor message from node $A$. Node $E$ should calculate its sending deferment according to the same rule. In order to cope with the loop problem, node $E$ should wait for an additional delay before initiating its transmission. In general, if a node is not a one-hop neighbor of an anchor node, it should wait for an additional period before forwarding the anchor's message. Suppose all nodes that need to broadcast are located within a ring characteristiced by two circles with radius $\alpha \times R$ and $R$, where $\alpha$ is determined by the node density obtained by overhearing. As an example, in Figure 5.1, $C$ may not need to broadcast if there are many nodes located within the ring determined by two circles with radius $0.5R$ and $R$. The additional

delay is then calculated with a $Pr$ value that is expected at the $0.5R$ distance. Simulation results show that in our proposed backoff-based flooding, all nodes broadcast only once.

### 5.1.2 Positioning via Particle Filtering

For the positioning step, due to location uncertainty inserted by mobility, a node inserts virtual anchors to aid on constraining the localization error. Let $(X_i, Y_i)$ be the coordinates of a virtual anchor node, where $i = \{1, 2, 3, \cdots, M\}$. Here, we select the midpoint of two one- or two-hop neighbor nodes as the position of virtual anchor node as shown in Fig. 5.2. Note that a node can estimate its distance to an anchor node and other regular nodes using the effective average hop distance and the number of hops in-between. These distances are used to constrain a small prediction area, from which particles are drawn and filtered.As shown in Fig. 5.2, the gray rectangle indicates the prediction area from where particles representing possible locations are extracted. The node's current velocity is also used to minimize the prediction area. The speed information can be collected from sensor data. For instance, sensor nodes are able to estimate their velocities using a three-dimensional accelerometer. As shown in Fig. 5.2, a regular node $k$

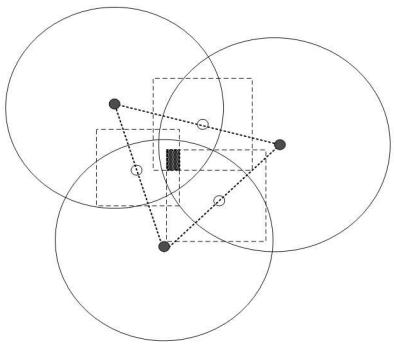

FIGURE 5.2: Building the prediction box.

located at the center of the intersection area is able to directly communicate with three one-hop neighbors. For each pair of one-hop neighbors, a virtual anchor node $i$ is created and $k$ builds a square of size $2 * d_{eff}^{k,i}$ centered at $i$, $d_{eff}^{k,i}$ being the estimated distance between $k$ and $i$. Based on the current velocity of sensor node, the coordinates of the reduced sampling rectangle area are calculated as follows:

$$
\begin{aligned}
x_{min} &= \max(\max_{i=1}^{n}(X_i - d_{eff}^{k,i}), x_{t-1} - v_t) \\
x_{max} &= \max(\min_{i=1}^{n}(X_i + d_{eff}^{k,i}), x_{t-1} - v_t) \\
y_{min} &= \max(\max_{i=1}^{n}(Y_i - d_{eff}^{k,i}), y_{t-1} - v_t) \\
y_{max} &= \max(\min_{j=1}^{n}(Y_i + d_{eff}^{k,i}), y_{t-1} - v_t),
\end{aligned}
$$

where $(X_{t-1}, Y_{t-1})$ are the coordinates of particle $l_{t-1}$. When we consider two-hop neighbors, we replace $d_{eff}^{k,j}$ with the estimated distance between regular node $k$ and its two-hop neighbor virtual anchor nodes. Based on Fig. 5.3, let the distance between anchor nodes $A$ and $B$ be $d_2$,

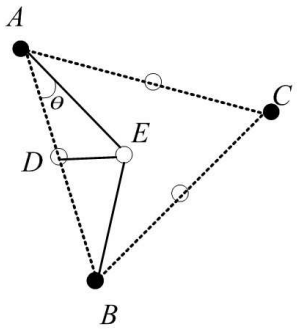


FIGURE 5.3: System model

the distance between $A$ and regular node $E$ be $d_1$ and the distance between regular node $E$ and anchor node $B$ be $d_3$. The distance between the virtual anchor node $D$ and regular node $E$ is defined as $d_0$. Finally, $\theta$ is the angle between line segments $\overline{AB}$ and $\overline{AE}$, which can be calculated from the cosine rule. After obtaining the values of $d_1$, $d_2$ and $d_3$ from triangle $\triangle ABE$, we have:

$$\cos\theta = \frac{d_2^2 + d_1^2 - d_3^2}{2d_1d_2}. \tag{5.7}$$

Similarly, in triangle $\triangle ADE$, we have:

$$\cos\theta = \frac{(d_2^2/4) + d_1^2 - d_0^2}{d_1d_2}. \tag{5.8}$$

Thus, we can calculate the value of $d_0$ based on eqs. (5.7) and (5.8) as follows:

$$d_0 = \frac{\sqrt{2d_1^2 + 2d_3^2 - d_2^2}}{2}. \tag{5.9}$$

**Prediction Phase** If the anchor's distance and speed constraint are disjointed, for example at initialization time, the node excludes the speed constraint when calculating the prediction area. The prediction area helps to draw valid particles in the prediction phase. The probability of a given current location based on a previous estimate is given by the uniform distribution:

$$p(L_t|L_{t-1}) = \begin{cases} 1 & \text{if } x_{min} \le x_t \le x_{max} \cap y_{min} \le y_u \le y_{max} \\ 0 & \text{otherwise,} \end{cases} \tag{5.10}$$

where $(x_t, y_t)$ are the coordinates of particle $l_t$.

**Filtering Phase**

In the prediction phase, each node generates a set of uniformly distributed random values inside the prediction area. If the drawn particles are located inside the communication range of every neighbor, the node saves this position for the final estimation. Otherwise, the node discards it and repeats the prediction phase. The entire filtering phase in a node can be represented as follows:

$$\begin{aligned} filter(l_t) = \forall a \in M, d(l_t, a) \leq r + v_t \cap \\ \cap \forall b \in M, r - v_t \leq d(l_t, b) \leq 2r + v_t, \end{aligned}$$

where $l_t$ is the concerned particle, $M$ and $N$ are the sets of one-hop and two-hop neighbors, respectively, $r$ is the nodes radio range, $d(l_t, a)$ is the distance between particle $l_t$ and neighbor $a$, and $v_t$ is the current velocity of a neighbor node. After obtaining a sufficient number of valid particles, the final location estimate is calculated as the average of the particle set.

## 5.2 Lower Bound on the localization error

Nagpal *et al.* [34] have proposed a lower bound for the localization error in any range-free localization algorithm in static sensor networks where the sensors only use the connectivity information of the anchors within their first-hop neighborhood. However, there is a problem related to the analysis mentioned in their method since we cannot simply compute the average distance a sensor can move without changing the connectivity along a fixed direction. Inspired from their work, we derive a lower bound on the localization error in our algorithm as following.

Let the continuous variable $Z$ denote the maximum distance that a sensor can be moved without changing its neighborhood. Then, the expected value $E(Z)$ is a lower bound on the localization error of sensors. As Fig. 3 illustrates, a sensor located on the circle of $r$ can move distance $z$ without changing its connectivity if there is no sensor in the region $A(z)$, which is consist with the annular region between the circles $r$ and $r + z$ and the circle $z$.

The probability that $Z < z$ is equal to the probability that there is at least one sensor in the annular region between the circles $r$ and $r + z$ and the circle $z$ as shown in the Fig. 3. Thus, we have

$$F[Z] = \Pr(Z \leq z) = 1 - e^{-\rho A(z)} \tag{5.11}$$

where $\rho$ is equal to $N_s/A$ in which $A$ is the total area of the network region and $N_s$ is the total number of sensors in area A.

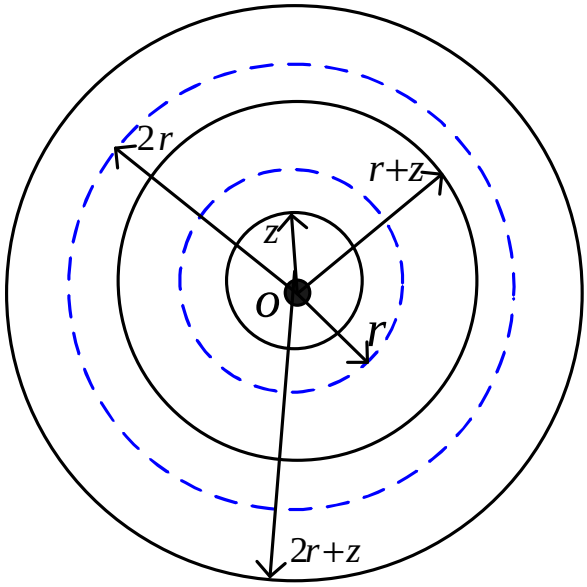


FIGURE 5.4: Move distance on impact of connectivity

The area $A(z)$ is given as

$$\begin{aligned} A(z) &= \pi(2r+z)^2 - \pi(2r)^2 + \pi z^2 \\ &= 2\pi z^2 + 4\pi rz. \end{aligned} \tag{5.12}$$

The probability density function of $Z$ is given as

$$f[z] = (4\rho\pi z + 4\rho\pi r)e^{-\rho(2\pi z^2+4\pi rz)}. \tag{5.13}$$

Therefore, $E(Z)$ can be calculated as:

$$\begin{aligned} E[Z] &= \int_0^r z \cdot f(z)dz \\ &= \int_0^r (4\rho\pi z^2 + 4\rho\pi rz) \cdot e^{-\rho(2\pi z^2+4\pi rz)}dz \\ &= 4\rho\pi \left\{ \begin{array}{l} \dfrac{1}{2(2\rho\pi)^{\frac{3}{2}}}\gamma\left(\dfrac{1}{2}, 2\rho\pi r^2\right) + \dfrac{r}{4\rho\pi}\gamma\left(1, 2\rho\pi r^2\right) \\ + \dfrac{1}{(4\rho\pi r)^3}\gamma\left(3, 4\rho\pi r^2\right) + \dfrac{r}{(4\rho\pi r)^2}\gamma\left(2, 4\rho\pi r^2\right) \end{array} \right\} \end{aligned} \tag{5.14}$$

where $\gamma(x, y)$ is the incomplete Gamma function.

## 5.3 Performance Evaluation

The general performance of our algorithm was obtained through simulation, using an adapted version of the simulator provided by the authors of MCL [22]. We evaluated the effectiveness of the backoff-based broadcast mechanism and the location accuracy of our proposal in terms of node speed, node density, anchor density, and communication irregularities, and compared it to four other algorithms: Centroid, Gradient, MCL, and MCB.

For the following results, we consider a topology of 320 nodes, placed in a random uniform manner over an area of $500 \times 500$ square units. Unless specified otherwise, we consider an anchor density of 1, node density of 10, and radio propagation using the unit disk model. These parameters were also varied and their evaluation can be seen in the next subsections. The radio range was set to 50 units and the maximum speed to 50 units per time interval. Anchor and regular nodes move using a modified version of the random waypoint model, with no pauses between intervals in order to prevent the average speed decay problem [9].

In the case of MCL-based algorithms (MCL, MCB, and our approach), we used a fixed sampling set of 50 units. Just like [22], we have verified that this is the best cost-benefit solution. While maintaining more samples improves accuracy, it also increases computational overhead and memory requirements. For each parameter, a set of 30 simulation runs was performed and results were averaged.

### 5.3.1 Evaluation of the Broadcast Mechanism

We investigate the effectiveness of the backoff-based broadcast mechanism which is adopted in step 1 of our proposal. Fig. 5.5 shows the number of beacon messages an anchor node needs to broadcast using simple flooding and our proposed backoff-based flooding to guarantee node localization. Nodes are ordered in increasing distance to the anchor node located at the left bottom corner. The minimum hop count of the farthest node to the anchor is 9. We can observe that some nodes have to broadcast the same related message up to *five* times in simple flooding. Generally, the farther away a node is from the anchor node, the more messages it needs to broadcast to correct the accumulated error. In contrast, in our proposed backoff-based flooding all nodes obtain their correct minimum hop counts with an overhead of one message per node. Therefore, our design effectively reduces the number of redundant messages. In another experiment, we distribute 200 nodes in a $500m \times 500m$ field and vary the transmission range from 100 to 50 meters. The average total number of anchor messages used by all nodes is presented in Fig. 5.6. In general, as the transmission range decreases, the accumulated error increases. Distant nodes need to rebroadcast more times. A transmission range less than 60 meters cannot

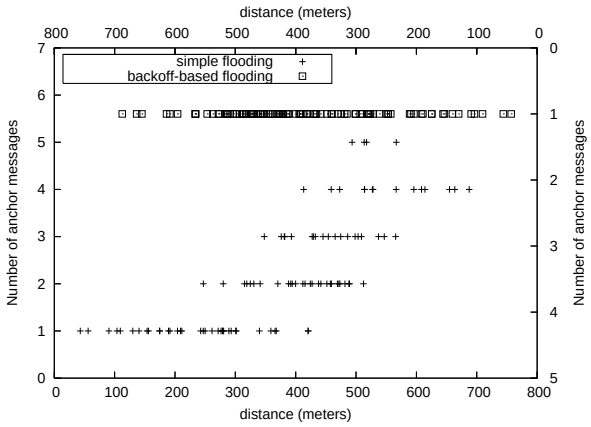


FIGURE 5.5: Number of anchor messages transmitted per node

ensure connectivity and thus the overhead decreases suddenly. Fig. 5.6 shows that our algorithm scales well to network size and substantially suppresses redundant broadcasts.

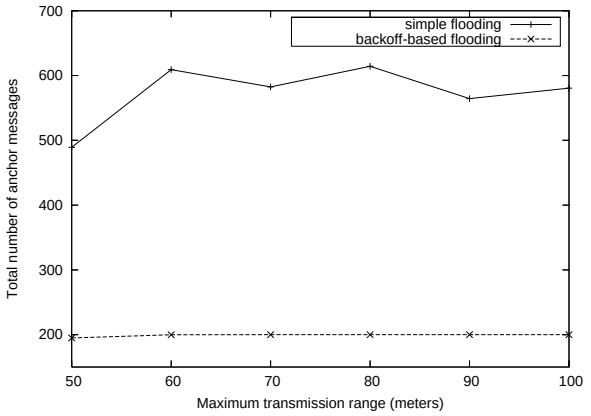


FIGURE 5.6: Average number of anchor messages used by all nodes

### 5.3.2 Convergence Time

The second simulation analysis concerns the location accuracy convergence. As it can be seen from Fig. 5.7, the initial sharp decline on the estimation error curves of the MCL-based algorithms is due to new location announcements from anchors being incorporated into the sequential Monte Carlo process. This is followed by a stable phase declaring the balance between updates to the posterior location distribution and uncertainty introduced by mobility. MCB and our proposal give similar performance, though the latter achieves slightly better accuracy. This is due to a smaller sampling area, which effectively speeds up the collection of valid samples, and also due to the optimized filtering phase, which uses actual sensor data for constraining the filtering area, opposed to a theoretical maximum velocity boundary. Centroid and Gradient do not exploit position history information, so their accuracy does not change over time.

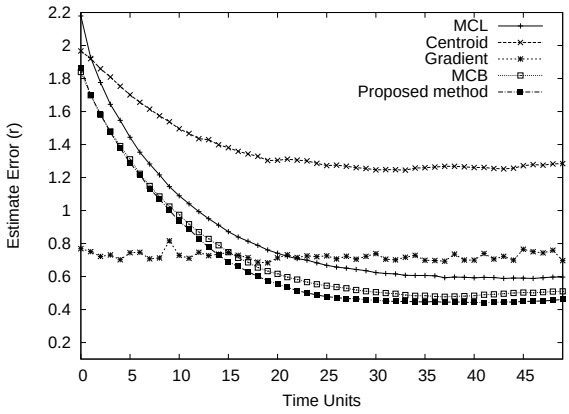


FIGURE 5.7: Accuracy comparison

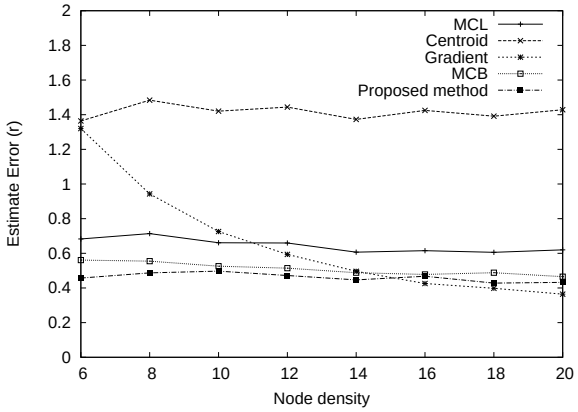


FIGURE 5.8: Impact of node density

### 5.3.3 Node density

Fig. 5.8 shows the impact of node density variation on the accuracy of each algorithm while the anchor density is kept constant. Centroid and the MCL-based algorithms are slightly affected by node density. In the case of the MCL-based algorithms, even when there are only two-hop anchor neighbors, enough samples can be filtered to obtain a decent location estimate. For Gradient, a higher density of nodes reduces the estimation error of the hop size leading to a higher accuracy as well. In our simulation experiments, Gradient performs best when the node density is over 16.

### 5.3.4 Anchor density

Increasing anchor density facilitates the retrieval of location information by regular nodes. Fig. 5.9 shows the average estimate error of different localization algorithms when the anchor density varies. We can see that all MCL-based algorithms take advantage of a higher anchor density, as more position announcements will be available for filtering. The same happens to

Centroid. In the case of Gradient, the impact over accuracy is negligible as information from the whole network is used independent of the number of anchors available. Our proposal performs better than the other algorithms for reasons explained above (smaller sampling area and better filtering technique).

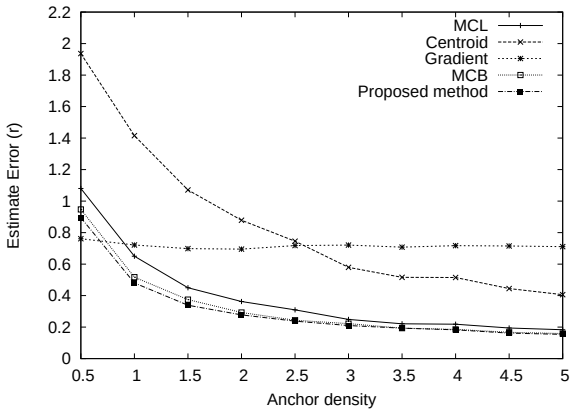


FIGURE 5.9: Impact of anchor density

### 5.3.5 Node speed

As we can see from Fig. 5.10, for all the MCL-based algorithms the maximum speed variation does not affect much the location accuracy. At higher speeds, nodes hear new anchors more often which add new information to the filtering phase, keeping the sample set updated. On the other hand, as larger distances are traversed at each time unit, the sampling area becomes larger, decreasing the algorithm's accuracy. In the case of Gradient, it is assumed that all network information is provided to every node at each time unit, a condition that is too optimistic for a real network. Therefore, node speed also does not affect its performance. Still, it can be seen that its estimation error is higher than the MCL-based algorithms. Node speed also does not affect Centroid.

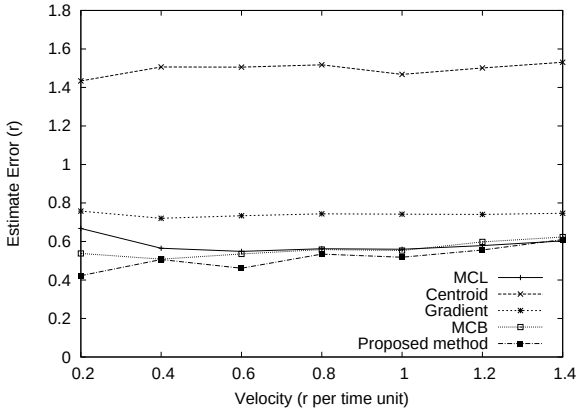


FIGURE 5.10: Impact of node speed

### 5.3.6 Communication Irregularities

Although the unit disk model is a simple and easy-to-use communication framework, it does not reflect the reality of wireless communication. The measured signal strength of radios can vary substantially with environmental conditions and antenna irregularities. This also affects the localization accuracy. Although many complex studies on radio propagation models have been proposed, we decided to use the Degree of Irregularity (DoI) [19] to model transmission and reception adversities for comparison purposes. The DoI parameter defines the radio signal strength variation on each direction of radio propagation. As its value increases, multihop communication is affected and the localization error of every algorithm increases, except for Centroid, as shown in Fig. 5.11. We can see from the results that our proposed algorithm degrades more gracefully. Despite the message exchange hardships, our proposal is still able to filter a larger number of valid samples than the other MCL-based algorithms.

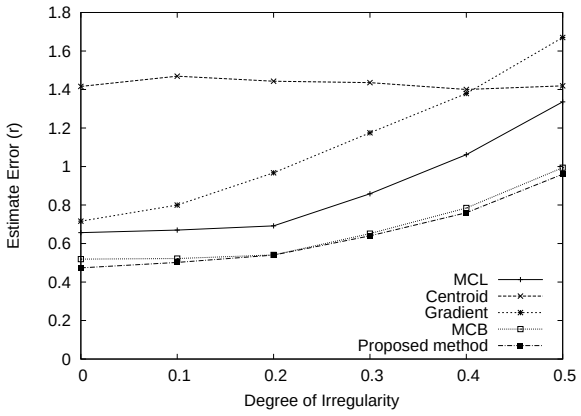


FIGURE 5.11: Impact of communication irregularities

## 5.4 Summary

We present a distributed hop distance measurement and particle filter-based cooperative localization algorithm for mobile WSNs. Our proposal is scalable, robust, and self-adaptive to the dynamics of a mobile sensor network. Our proposed algorithm can reduce the hop distance estimation error accumulated over multiple hops by using a differential error correction scheme. In order to efficiently suppress redundant broadcasts and to reduce communication overhead, a backoff-based broadcast mechanism is proposed. It also improves localization performance by including particle filtering technology. Simulation results show that the proposed algorithm achieves better performance than other state-of-the-art algorithms. Influence of physical obstacles over the communication model remains to be explored as future work.

# Chapter 6

# Distributed Source Localization in Wireless Underground Sensor Networks

In the previous chapters, we have studied range-free localization problems. Herein, we focus on range-based method in wireless underground sensor networks. Considering the requirement of the application area, the designed localization algorithm is more practical. Node localization plays an important role in many practical applications of wireless underground sensor networks (WUSNs), such as finding the locations of earthquake epicenters, underground explosions, and microseismic events in mines. It is more difficult to obtain the time-difference-of-arrival (TDOA) measurements in WUSNs than in terrestrial wireless sensor networks because of the unfavorable channel characteristics in the underground environment. The robust Chinese remainder theorem (RCRT) has been shown to be an effective tool for solving the phase ambiguity problem and frequency estimation problem in wireless sensor networks. In this paper, the RCRT is used to robustly estimate TDOA or range difference in WUSNs and therefore improves the ranging accuracy in such networks. After obtaining the range difference, distributed source localization algorithms based on a diffusion strategy are proposed to decrease the communication cost while satisfying the localization accuracy requirement. Simulation results confirm the validity and efficiency of the proposed methods.

## 6.1 Introduction

Wireless underground sensor networks (WUSNs) are an important extension of terrestrial wireless sensor networks, as they can be used for estimating the locations of earthquake epicenters, underground explosions, microseismic events in mines, etc. Normally, the sensor nodes in

WUSNs are buried underground and exchange information wirelessly via the dispersive underground channel. Some experimental results with WUSNs are reported in [42].

In terrestrial wireless sensor networks, time difference of arrival (TDOA) has been widely used for node localization [31]. Because of the physical characteristics of the dispersive underground channel and the heterogeneous network architecture of WUSNs, source localization for WUSNs based on TDOA is much more complicated and challenging than that in terrestrial wireless sensor networks [51]. In a dispersive medium, we cannot directly obtain the range differences between the source and sensors from TDOA measurements since the propagation velocity is a function of frequency due to the fact that different frequency components have different propagation speeds [11].

Knowing the location of sensor nodes is important in many practical applications of wireless underground sensor networks. The objective of a positioning system is to determine accurate node locations with low complexity and communication cost. Localization algorithms for traditional terrestrial wireless sensor networks can be mainly classified into two types: range-based methods and range-free methods. Range-based methods usually have higher location accuracy than range-free ones while demanding additional hardware cost.

In [63], a distributed TDOA estimation method that relies only on radio transceivers without other auxiliary measurement equipment was presented. Ultra-wideband (UWB) signaling can be used to accurately achieve time of arrival (TOA) or TDOA measurements, which has the advantages of low-cost and penetrating ability, but also has the weakness of short-range. TDOA based algorithms provide high localization accuracy, and represent a practical method for estimating range differences and source positions in WUSNs. However, this method also faces many challenges. In particular, limited range and directionality constraints decrease the accuracy of range difference estimation. We notice that the TDOA can usually be obtained from the measurement of a signal's phase which is susceptible to phase ambiguity problems. The Chinese remainder theorem (CRT) offers a closed-form analytical algorithm to calculate a dividend from several of its corresponding divisors and remainders, and can be applied to solve the ambiguity problem here. In our ranging application, the remainders in the CRT are the measured "remainder" wavelengths, the divisors are the measuring wavelengths, and the dividend is the range difference to be estimated. However, directly using the CRT is not feasible due to its over-sensitivity to noise, i.e. a small error in a remainder can lead to very large error in the estimated dividend. To avoid this weakness of the CRT, we further propose to use a robust Chinese remainder theorem (RCRT) algorithm to estimate the range difference, in which the dividend can still be reconstructed with only a small error if the errors on remainders are bounded within a certain level [28]. As a result, the range differences or TDOAs can be robustly estimated from noisy measurements in WUSNs by using the RCRT.

After obtaining the range differences using the RCRT, we can estimate the source position based on statistical signal processing methods. For traditional terrestrial wireless sensor networks, TDOA based localization algorithms are normally implemented in a centralized way. In the centralized solution, all nodes relay their TDOA measurements to a fusion center, which uses a conventional localization algorithm to obtain the source position, and then sends the global estimate back to every node. This strategy requires a large amount of energy for communications [10] and has a potential failure point (the central node). Distributed strategies are an attractive alternative, since they are in general more robust, require less communications, and allow for parallel processing. To address this limitation of centralized processing, we propose distributed source localization algorithms using a diffusion strategy in this paper. Diffusion algorithms are applicable to distributed implementations since nodes communicate in an isotropic manner with their one-hop neighbor nodes, and no restrictive topology constraints are imposed. Thus the algorithms are easier to implement and are also more robust to node and link failures, at the expense of inferior performance compared to incremental or centralized solutions. However, this approach allows nodes to obtain better estimates than they would without cooperation.

The rest of the paper is organized as follows: Section 6.2 establishes the mathematical model of the problem, and derives the proposed ranging method based on the RCRT. Section 6.3 gives the distributed source localization algorithm based on the diffusion strategy. Simulation results are given in Section 6.4, and conclusions are drawn in Section 6.5.

## 6.2 System model and TDOA estimation via the robust CRT

Due to the large attenuations in underground environments, experimental results show that underground to underground (UG2UG) communication is not feasible at the 2.4GHz frequency band [49]. Underground communication becomes practical only at lower frequencies. As reported in [43] and [44], a WUSN system operating at 433MHz with a maximum transmit power of +10dBm usually achieves a communication range of around one meter for UG2UG communication and more than 30m for underground to aboveground (UG2AG) communication. These communication ranges have already exceeded the wavelength of the transmitted signal, which results in phase ambiguity when the distance difference is directly calculated from the phase. In this section, we first propose a method based on the robust CRT to resolve this phase ambiguity when computing the range distance.

Consider a WUSN with $L$ sensor nodes at known positions $(x_i, y_i)$, $i = 1, 2, \ldots, L$, receiving a signal from a source at an unknown position $(x, y)$ through a dispersive medium, as shown in Fig. 6.1. Of course, the distance between the source and the $i$-th sensor is $R_i = \sqrt{(x_i - x)^2 + (y_i - y)^2}$. The range difference (RD) between the $i$-th and $j$-th receivers, denoted as $r_{i,j}$, is then $r_{i,j} = R_i - R_j$.

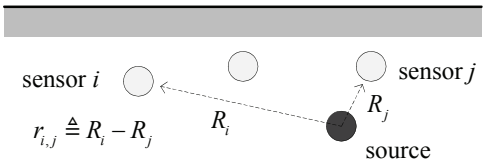


FIGURE 6.1: System model for WUSN localization.

If the medium is non-dispersive, the propagation delay for any frequency is constant. However, in a dispersive medium, the signal propagation velocity is a function of the signal's frequency, denoted by $v(\omega_k)$ for frequency $\omega_k$; that is, the propagation delay is frequency dependent. We denote the delay of propagation at frequency $\omega_k$ for sensor $i$ as $t_i^k = \frac{R_i}{v(\omega_k)}$.

We assume that the source transmits a sinusoid signal $s^k(t) = e^{j\omega_k t}$ at frequency $\omega_k$. Then, the $i$-th sensor receives the signal as

$$\begin{aligned} s_i^k(t) =& s^k(t - t_i^k) + n_i(t) \\ =& e^{j\omega_k(t-t_i^k)} + n_i(t), \end{aligned} \tag{6.1}$$

where $n_i(t)$ is the noise at sensor $i$, and $\{n_i(t)\}, i = 1, 2, \ldots, L$ are independent white Gaussian noise processes. Similar to that of sensor $i$, the received signal at sensor $j$ is

$$s_j^k(t) = e^{j\omega_k(t-t_j^k)} + n_j(t). \tag{6.2}$$

By taking the cross-correlation of $s_i^k(t)$ and $s_j^k(t)$, we have

$$I_{ij}^k = \frac{\int_0^T [s_i^k(t)]^* s_j^k(t) dt}{T}. \tag{6.3}$$

It is easy to find that $I_{ij}^k$ is an unbiased estimator of $e^{j\omega_k(t_i^k - t_j^k)}$, for which it follows that

$$\lim_{T\to\infty} I_{ij}^k = e^{j\omega_k(t_i^k - t_j^k)} = e^{j\frac{\omega_k r_{i,j}}{v(\omega_k)}}, \tag{6.4}$$

where the range difference $r_{i,j}$ is contained in the phase of $I_{ij}^k$. We denote the phase of $I_{ij}^k$ as $\phi_{ij}(k)$, i.e.

$$\phi_{ij}(k) = \left(\frac{\omega_k r_{i,j}}{v(\omega_k)}\right) \bmod 2\pi. \tag{6.5}$$

One can determine $r_{i,j}$ from $\phi_{ij}(k)$. However, there are two issues of concern with this approach: 1) the value of $\phi_{ij}(k)$ is folded by $2\pi$ and 2) the measurements are noisy, i.e.

$$\frac{\omega_k r_{i,j}}{v(\omega_k)} = \phi_{ij}(k) + 2\pi b(k) + e(k), \tag{6.6}$$

where $b(k)$ is the folding integer, $e(k)$ is the noise for frequency $\omega_k$.

For issue 1, no matter how large the actual $r_{i,j}$ is, the RD $r_{i,j,k} = \phi_{ij}(k) \cdot v(\omega_k)/\omega_k$ converted directly from $\phi_{ij}(k)$ is always within one wavelength of the signal $\lambda_k = 2\pi v(\omega_k)/\omega_k$. Therefore, $r_{i,j}$ can not be determined uniquely by a single $\phi_{ij}(k)$. We add more constraints to confine the solution space by measuring the phase at different frequencies $\omega_k, k = 1, 2, \ldots, K$. The Chinese remainder theorem (CRT) provides a solution of evaluating a dividend from its remainders. We can regard $r_{i,j}$ as the dividend, $\lambda_k$ as the divider, and $r_{i,j,k}$ as the corresponding remainder, then evaluate $r_{i,j}$ via the CRT. It seems that the CRT gives a perfect solution to this problem. However, when we consider the measurement noise, the traditional CRT is not suitable because it is sensitive to noise. A small error in the remainder can result in a large error in the estimated dividend. Therefore, we adopt a robust CRT method [28]. Theorem 1 in [28] proves that the robust CRT can tolerate an error which is bounded by $\tau < M/4$, where $M$ is the greatest common divider (GCD) among the dividers. To be more specific, if all the remainder errors are not greater than the error bound $\tau$, the estimation error of the unknown dividend is upper bounded by $\tau$, i.e.

$$\left| r_{i,j} - \hat{r}_{i,j} \right| \leq \tau. \tag{6.7}$$

Based on this robust CRT, we provide the following solution to solve the problem:
Step 1. Estimate $\phi_{ij}(k)$ by calculating the phase of $I_{ij}^k$. Denoting the estimated phase as $\tilde{\phi}_{ij}(k) \in [0, 2\pi)$, and the corresponding distance converted from the phase is

$$\tilde{r}_k = \frac{\tilde{\phi}_{ij}(k)}{2\pi}\lambda_k \quad \in [0, \lambda_k), k = 1, ..., K. \tag{6.8}$$

Note that the CRT is commonly expressed in the integer ring while the distance is a real number. Therefore, we extend the algorithm from the integers to the reals by introducing a real common factor among the divisors. We assume that $\lambda_k, k = 1, ..., K$ have a real common factor of $M$ which satisfies

$$\lambda_k = M\Gamma_k, \tag{6.9}$$

where $\Gamma_k$ are still co-prime integers, i.e. $(\Gamma_m, \Gamma_n) = 1$, for $1 \leq m, n \leq K, m \neq n$, and $(\cdot, \cdot)$ denotes GCD. According to the passages mentioned above, we have the following equation:

$$\begin{aligned} r_{i,j} &= n_k\lambda_k + r_k \\ &= n_k\lambda_k + \tilde{r}_k + \Delta r_k \end{aligned}, k = 1, ..., K, \tag{6.10}$$

where $n_k$ are the corresponding quotients (folding integers), $\Delta r_k$ denotes the measurement errors of $\tilde{r}_k$ with $|\Delta r_k| < \tau$, when $\tau$ is the error bound.
Step 2. For notational convenience, define the following symbols:

$$\Gamma \triangleq \prod_{k=1}^{K} \Gamma_k, \tag{6.11}$$

$$\gamma_k = \Gamma/\Gamma_k. \tag{6.12}$$

Calculate and find the sets,

$$S_k \triangleq \left\{(\bar{n}_1, \bar{n}_k) = \arg \min_{(\hat{n}_1, \hat{n}_k) \in \Omega_k} |\hat{n}_k \lambda_k + \tilde{r}_k - \hat{n}_1 \lambda_1 - \tilde{r}_1| \right\}, k = 2, 3, ..., K, \tag{6.13}$$

where

$$\Omega_k \triangleq \{(\hat{n}_1, \hat{n}_k) | 0 \leq \hat{n}_1 \leq \gamma_1 - 1, 0 \leq \hat{n}_k \leq \gamma_k - 1\} \tag{6.14}$$

is the solution space of the quotients.

$S_k$ can be regarded as the optimal combination of the quotients $n_1$ and $n_k$ with which the difference of the estimated dividends achieves its minimum.
Step 3. Let $S_{k,1}$ denote the first element $\bar{n}_1$ of the 2-tuples,

$$S_{k,1} \triangleq \{\bar{n}_1 | (\bar{n}_1, \bar{n}_k) \in S_k \text{ for some } \bar{n}_k\}. \tag{6.15}$$

Calculate the intersection set of $S_{k,1}$:

$$S \triangleq \bigcap_{k=2}^{K} S_{k,1}. \tag{6.16}$$

In [28], Li *et al.* prove that if the error bound is less than $M/4$, the set $S$ contains only the true value of $n_1$, i.e. $S = \{n_1\}$. In addition, $n_k$ can also be determined from $S_k$, that is, if $(n_1, \bar{n}_k) \in S_k$, then $\bar{n}_k = n_k$ for $2 \leq k \leq K$. Therefore, with all the quotients being determined correctly, the error of the estimated $r_{i,j}$ is therefore bounded by $|\hat{r}_{i,j} - r_{i,j}| \leq \tau$, where $\hat{r}_{i,j}$ is obtained by averaging the estimations corresponding to different wavelengths, i.e.

$$\hat{r}_{i,j} = \frac{1}{K} \sum_{k=1}^{K} (n_k \lambda_k + \tilde{r}_k). \tag{6.17}$$

*Remark:* One may notice that to find the set $S_k$ in (6.13) we need to search among the possible values of $\Omega_k$, which is a 2-D searching with the order of $(\Gamma_2 \Gamma_3 ... \Gamma_L)^2$ and indeed requires a high computation complexity. However, the complexity can be decreased by using a fast algorithm proposed in [28] and [26] to a 1-D searching with the order of only $2(L-1)\Gamma_i$. One can easily apply the fast algorithm to the application in this paper. We do not describe this fast algorithm herein since this is not the focus of this paper.

## 6.3 Diffusion Algorithms for Source Localization

After obtainning the range differences using the RCRT, some localization algorithms can be used to estimate the source position. Herein, we propose an algorithm for source localization, which we term diffusion weighted least squares (WLS). To be fully distributed, this algorithm is diffusion-based. First, the nodes in the cluster will send their measurements to the cluster head. Then, the cluster head can give a local estimate using these measurements locally. After obtaining the local estimate, cluster heads will exchange these local estimates to achieve a diffusion estimate, which will be close to the global estimate. Before including the diffusion estimate, we first introduce the global WLS estimate in the next subsection, in which all of the measurements are sent to the fusion center for estimating the source location. Comparing with global estimation, no fusion center is required in our algorithms and estimates are obtained through local exchanges with neighbors only.

### 6.3.1 Global Weighted Least Square Problem

Consider a set of $N$ cluster heads and $K = MN$ sensor nodes (each cluster head is associated with $M$ sensor nodes) spatially distributed over some region with known locations $x_i$'s (we consider the 2-D Cartesian coordinate system). The objective of the network is to collectively estimate an unknown deterministic column vector - the location $x$ of a source. All the nodes (cluster heads and sensor nodes) in the network can measure the signal transmitted from the source. The sensor nodes transmit their measurements to the corresponding cluster head and each cluster head forms a set of $M$ TDOA measurements with itself being the reference. Then, cluster heads can send their TDOA measurements to the fusion center. The TDOA measurements are formed one at a time by comparing the signal from the cluster head and the signal from a sensor node, thus leading to uncorrelated estimates if the estimation period is longer than the typical coherence time of the mobile radio channel. Finally, the fusion center obtains altogether $K$ TDOA based range difference measurements $r_{i,j}$'s in the network.

The scalar model for TDOA based range difference is given by

$$r_{i,j} = \|x - x_i\| - \|x - x_j\| + n_{i,j}; \tag{6.18}$$

we stack all the $r_{i,j}$'s in a vector and obtain

$$r = s(x) + n$$

where $t = \text{col}\{r_{i,j}\}$, $s(x) = \text{col}\{\|x - x_i\| - \|x - x_j\|\}$ and $n = \text{col}\{n_{i,j}\}$. Each $r_{i,j}$ can be alternatively denoted as $[r]_l$ to reflect its location in vector $r$. The corresponding covariance matrix for $n$ is denoted as $W$ and $W = \text{diag}\{\sigma_1^2, \ldots, \sigma_K^2\}$.

The global weighted least squares estimator for estimating $x$ given $t$ is thus

$$\begin{aligned}\hat{x}_G &= \arg\min(r - s(x))^T W^{-1}(r - s(x)) \\ &= \arg\min \sum_{i=1}^{K} \sigma_i^2([r]_i - [s(x)_i])^2. \end{aligned} \tag{6.19}$$

Assuming the $n_{i,j}$'s are Gaussian, then the covariance of $\hat{x}_G$ attains the corresponding CRLB, which is given by [23]

$$\text{cov}(\hat{x}_G) = (P^T W^{-1} P)^{-1} \tag{6.20}$$

where

$$[P]_{i,j} = \frac{\partial [s(x)]_i}{\partial [x]_j}\Big|_{x=x_0} \tag{6.21}$$

and $x_0$ denotes the true position of the source.

For the TDOA measurements, $P$ is a $K \times 2$ matrix and the elements of $P$ are given by

$$\begin{aligned}[P]_{l,1} &= \frac{[x_i]_1 - [x]_1}{\|x_i - x\|} - \frac{[x_j]_1 - [x]_1}{\|x_j - x\|}\Big|_{x=x_0}, \\ [P]_{l,2} &= \frac{[x_i]_2 - [x]_2}{\|x_i - x\|} - \frac{[x_j]_2 - [x]_2}{\|x_j - x\|}\Big|_{x=x_0}\end{aligned}$$

where we assume $[s(x)]_l$ involves nodes (a sensor node and a cluster head) $i$ and $j$.

### 6.3.2 Local Weighted Least Squares Problem

For each cluster head $k$, it has access to limited data from its own and its neighbors. It can then solve the WLS problem locally as

$$\hat{x}_k = \arg\min \sum_{i=1}^{K} c_{i,k} \sigma_i^2([r]_i - [s(x)_i])^2 \tag{6.22}$$

where $c_{i,k}$'s are the associated weights for node $k$ and $c_{i,k} = 0$ if $[t]_i$ is not accessible for node $k$. Let $C$ denote the $K \times N$ matrix with elements $c_{i,k}$. We require $\mathbb{1}^T C = \mathbb{1}^T$. So that the estimation fusion method can use those local estimates to attain the performance of the global estimate [10], where $\mathbb{1}$ denotes a $N \times 1$ column vector with unity entries.

A local estimate can also be written as

$$\hat{x}_k = (P^T W^{-1} C_k P)^{-1} P^T W^{-1} C_k z \triangleq L_k z \tag{6.23}$$

where $C_k = \text{diag}\{Ce_k\}$ ($e_k$ is an $N \times 1$ vector with a unity entry in position $k$ and zeros elsewhere) and $z = r - s(x) + Px|_{x=x_0}$. $P$ can be estimated at $\hat{x}_k$.

The covariance matrix associated with $\hat{x}_k$ is given by $\text{cov}(\hat{x}_k) = L_k W L_k^T$. Here $L_k$ contains only local information due to the selection ability of $C_k$.

The estimation fusion method can then be used to fuse these local estimates in a distributed manner by utilizing the local covariance matrices as proper weights and the estimation fusion method can be shown to achieve the performance of the global estimation. However, it involves covariance estimation and matrix inversion.

### 6.3.3 Diffusion Algorithm

Besides estimator fusion, we can also use a diffusion algorithm to perform distributed estimation. For each cluster head $k$, at the $i$th time epoch, it exchanges its local estimate with its neighboring cluster heads and updates its local estimate using a diffusion algorithm

$$\hat{x}_{k,i} = \sum_{l=1}^{N} a_{l,k} \hat{x}_{l,i}, \tag{6.24}$$

where the $a_{l,k}$'s are the diffusion coefficients. Eq. (6.24) can be considered as a weighted average of the local estimates in the neighborhood of node $k$. Assume all the local estimates are unbiased. Then in order for $\hat{x}_{k,i}$ to be unbiased, we require $\mathbb{1}^T a_k = \mathbb{1}^T$ where $a_k = [a_{1,k}, \ldots, a_{N,k}]^T$. The diffusion process is repeated until all the local estimates have converged, i.e., $\|\hat{x}_{k,i+1} - \hat{x}_{k,i}\| \leq \epsilon \; \forall k$, where $\epsilon$ is a (small positive) design parameter.

One possible choice for the weights $a_{l,k}$ is to consider the degree of connectivity, which is

$$a_{l,k} = \begin{cases} \deg_l / \sum_{n \in N_k} \deg_n, & l \in N_k \\ 0, & \text{otherwise} \end{cases} \tag{6.25}$$

where $\deg_l$ denotes the cardinality of cluster head $l$'s neighbors (also cluster heads) and $N_k$ denotes the set of neighboring cluster heads of head $l$. Such choice has been observed to yield good results for the diffusion algorithm in general [10].

However, this method does not consider the reliability of different local estimates. The reliability of a local estimate is reflected in its associated covariance matrix. But estimating the covariance matrix is not an easy task for a nonlinear weighted least-squares estimator (WLSE). Here we propose a method for setting appropriate $a_{l,k}$'s which reflects the reliability of different local estimates to a certain extent without requiring use of the covariance matrices.

Since each local estimate contains certain errors, when sorting them in respective dimensions (each dimension of $\hat{x}_k$ is treated separately), the middle ones are more reliable. Therefore, for cluster head $k$, at the $i$th time epoch, it first finds the median $\tilde{x}_{k,i}$ along respective dimensions

among its received local estimates $\hat{x}_{l,i}$'s. Then for each obtained local estimate, head $k$ calculates $w^i_{l,k} = \exp(-\|\hat{x}_{l,i} - \tilde{x}_{k,i}\|^2/\gamma)$ if $l \in N_k$. Otherwise, $w^i_{l,k} = 0$. $\gamma$ is a parameter which controls how rapidly the weight decays as $\|\hat{x}_{l,i} - \tilde{x}_{k,i}\|$ grows. The diffusion coefficient $a^i_{l,k}$ is then set to

$$a^i_{l,k} = w^i_{l,k} / \sum_{j \in N_k} w^i_{j,k}. \tag{6.26}$$

Here we explicitly indicate the time epoch of $w^i_{l,k}$ and $a^i_{l,k}$ in the superscript. It can be seen that the larger the deviation between a local estimate $\hat{x}_{l,i}$ and $\tilde{x}_{k,i}$, the smaller the weight assigned to this local estimate and vice versa. Obviously, $\mathbb{1}^T a^i_{l,k} = \mathbb{1}^T$.

Another method of interest is to use an optimization technique. That is, to set $a_{l,k}$'s such that the trace of the covariance matrix of $\hat{x}_{k,i}$ is minimized. We start by examining the first time epoch $i = 1$. Then, we have

$$\hat{x}_{k,i} = \sum_{l=1}^{N} a^i_{l,k} \hat{x}_{l,i} = \sum_{l=1}^{N} a^i_{l,k} L_{l,i} z \tag{6.27}$$

where we have used (6.23).

The covariance matrix of $\hat{x}_{k,i}$ is thus given by

$$\mathrm{cov}(\hat{x}_{k,i}) = (\sum_{l=1}^{N} a^i_{l,k} L_{l,i}) W (\sum_{l=1}^{N} a^i_{l,k} L_{l,i})^T \tag{6.28}$$

and its trace is

$$\mathrm{tr}(\mathrm{cov}(\hat{x}_{k,i})) = \sum_{m,n=1}^{N} a^i_{m,k} a^i_{n,k} \mathrm{tr}(W L^T_{m,i} L_{n,i}) = (a^i_k)^T Q a^i_k \tag{6.29}$$

where $a^i_k = [a^i_{1,k}, \ldots, a^i_{N,k}]^T$ and $[Q]_{m,n} = \mathrm{tr}(W L^T_{m,i} L_{n,i})$. To be unbiased, we also require $\mathbb{1}^T a^i_k = \mathbb{1}^T$.

Therefore, to find the optimal $a^i_k$ in the sense of minimizing the diffusion covariance matrix, we need to solve an optimization problem:

$$\hat{a}^i_k = \arg\min (a^i_k)^T Q a^i_k, \ s.t. \ \mathbb{1}^T a^i_k = \mathbb{1}^T, \ a^i_k \geq 0, \ a^i_{l,k} = 0 \ \forall \ l \notin N_k. \tag{6.30}$$

This problem is convex if $Q \succ 0$ and thus can be solved fast and efficiently.

After determining $\hat{a}^i_k$ at time epoch $i$, $L_{l,i+1}$ is updated as $L_{l,i+1} = \sum_{l=1}^{N} \hat{a}^i_{l,k} L_{l,i}$ and $Q$ will also be updated accordingly. Then the above optimization process can be performed iteratively until estimates converge.

This optimization method can enhance the distributed fusion performance at the cost of slightly higher computational complexity compared with simply setting $a_{l,k}$ according to (6.25).

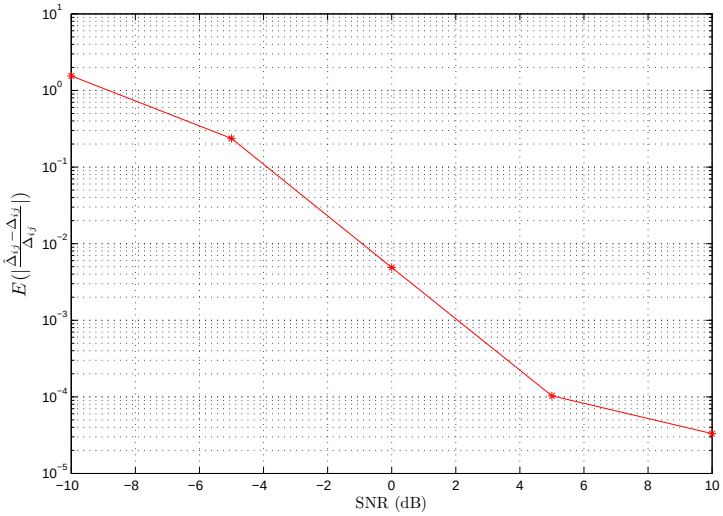


FIGURE 6.2: Relative estimation error decreases with increasing SNR.

To decrease the computational cost, the optimization process can be implemented only once for the first diffusion at each node, and the weight $a_k$ remains the same for the latter diffusions. Since after one diffusion, the updated local estimates becomes much less dissimilar and thus the weights will have much less influence on the followed diffusions.

## 6.4 Simulation results

In this section, simulation results are given. We first study the ranging performance using the RCRT in Subsection *6.4.1*. Then, the localization accuracy is introduced in Subsection *6.4.2*.

### 6.4.1 Ranging Performance

Assume that the signals are transmitted at 3 frequencies, i.e. $K$=3, $M$=80, $\Gamma_k$={15, 16, 17}, and the corresponding three dividers are $M_k$={1200, 1280, 1360} which represents the wavelengths of $\lambda_k$ = {120, 128, 136}mm. According to the RCRT, the maximum estimation distance is $d_{\max} = M \prod_{k=1}^{K} \Gamma_k$=32640mm. Each trial of simulation generates a random integers $r_{i,j}$, which is uniformly distributed in $[0, d_{\max}]$. And there are 1000 trials for each SNR. The result is shown in Fig. 6.1.

Then we consider the effect of $M$ on the performance. We set $M$ = 100, 200, 300, respectively and fix $\Gamma_k$={7,9}. The result is shown in Fig. 6.2 with 10000 trials for each SNR. According to the result, changing $M$ does not have significant influence on the relative error of distance estimation.

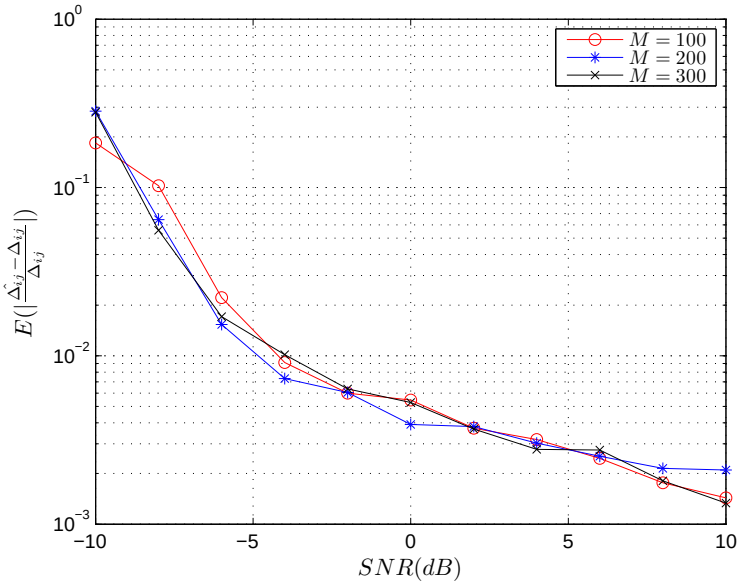


FIGURE 6.3: Comparison between the relative estimation errors for different values of $M$.

Next, we compare the performance under different values of $\Gamma_k$ with constant $M$ and $K$. In the simulation, we fix $M$=50, $K$=3, and let $\Gamma_k$ be $\{7, 11, 15\}$, $\{29, 33, 37\}$, $\{53, 57, 61\}$, respectively. Fig.6.3 demonstrates that the estimation error increases with $\Gamma_k$. The results from Fig. 6.2 and Fig. 6.3 can be explained by equations (6.8) and (6.9): the phase measurement error is amplified by $M$ and $\Gamma_k$, i.e. the error of $\tilde{r}_k$ is $\Delta r_k = \frac{\Delta\tilde{\phi}_{ij}(k)}{2\pi} M\Gamma_k$, where $\Delta\tilde{\phi}_{ij}(k)$ denotes the phase measurement error of $\tilde{\phi}_{ij}(k)$. The larger $\Gamma_k$ is, the larger error results. However, $M$ does not affect the performance because the robustness of the algorithm also linearly increases with $M$ which cancels the performance deterioration of the increased $M$. (The error tolerance of the algorithm is $\tau < M/4$)

In addition, we consider the scenario in which different sets of $\Gamma_k$ are compared under the constraint of constant maximum range $d_{\max} = M \prod_{k=1}^{K} \Gamma_k$. In Fig. 6.4, We choose $\Gamma_k$=$\{7, 11, 15\}$, $\{5, 11, 21\}$, $\{3, 11, 35\}$, respectively. The simulation results suggest that the performance is better if the differences between the $\Gamma_k$ are smaller.

Fig. 6.5 demonstrates that using more wavelengths results in better ranging performance. In this simulation, we fix the maximum estimation distance $d_{\max}$, and vary $K$. We consider the cases when $K$=2,3,4, respectively, with $M$=50 and $d_{\max}$=3465mm. $\Gamma_k$ are set to $\{33, 35\}$, $\{7, 11, 15\}$, $\{3, 5, 7, 11\}$, respectively. Simulation results demonstrate that our RCRT based ranging scheme can estimate the range differences with high accuracy.

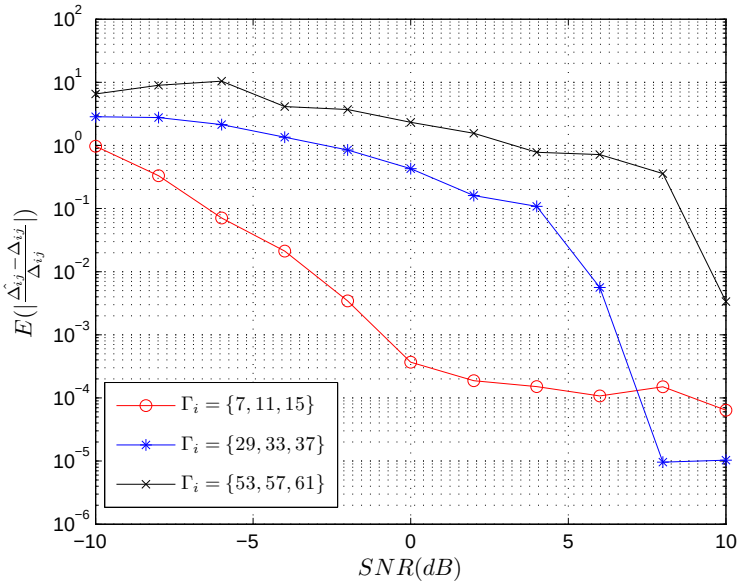


FIGURE 6.4: Comparison of the relative estimation error for different values of $\Gamma_k$, when $M$ and $K$ are fixed.

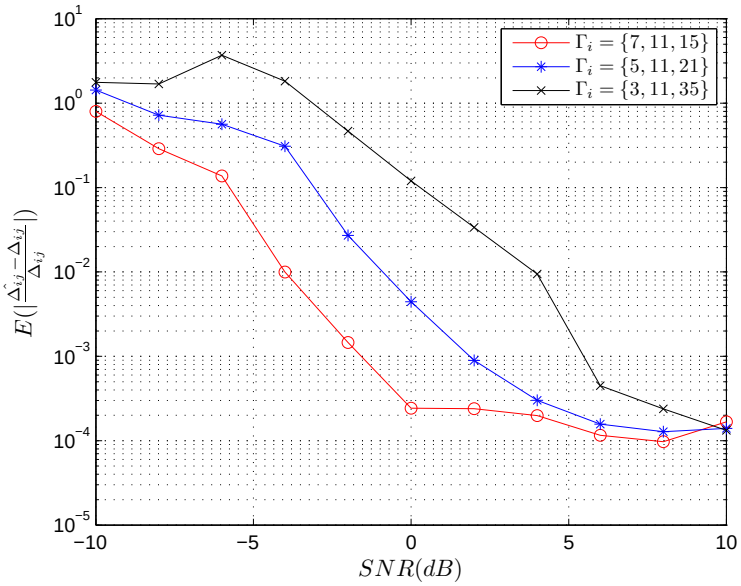


FIGURE 6.5: Comparison of the relative estimation error for different values of $\Gamma_k$, with $M$, $K$ and $d_{\max}$ fixed.

### 6.4.2 Comparison Results for Distributed Source Localization

We now show simulation results for source localization. The algorithms compared are: 1) *Global*: the global weighted least square estimator (6.19), 2) *Diff (con)*: the diffusion algorithm with coefficients set by considering connectivity (6.25), 3) *Diff (wei)*: the diffusion algorithm with coefficients set by weighting (6.26), 4) *Diff (opt)*: the diffusion algorithm with coefficients set by optimization (6.30) and 5) *Local*: simple average of all the local estimates, i.e., $\sum_{k=1}^{N} \hat{x}_k/N$.

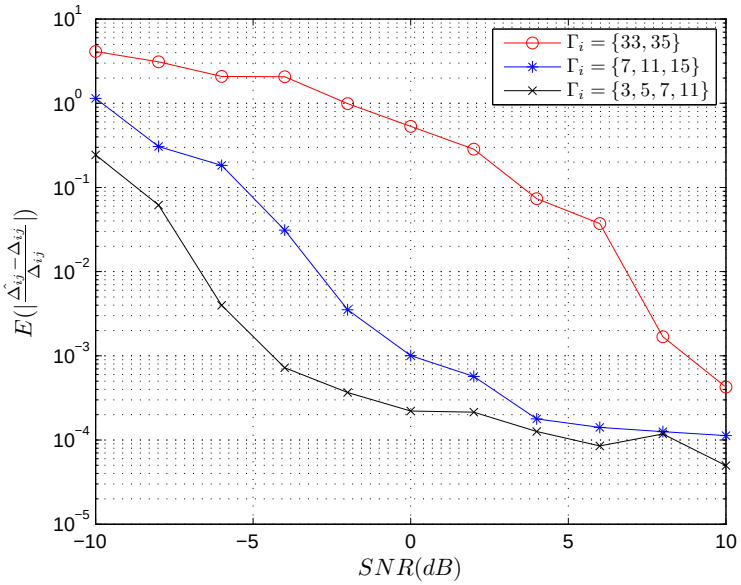


FIGURE 6.6: Comparison of the relative estimation error for different values of $K$.

The root mean square error (RMSE) is used as a performance metric, which is defined as $\sqrt{E(\|\hat{x} - x\|^2)}$. The Cramer-Rao Lower Bound (CRLB) on the RMSE based on the entire data (equals to $\sqrt{\text{tr}(\text{cov}(\hat{x}_G))}$ for Gaussian measurement noise) is also presented as a benchmark. Each simulated point is averaged over 200 runs.

The simulated network consists of $N$ cluster heads that are regularly deployed at grid points. The distance between neighboring cluster heads is set to 50 (the units are meters, here and below). Each cluster head has $M$ associated sensor nodes which are distributed uniformly around the corresponding cluster head. The source location is fixed at $[60, 70]$ in all the simulations. The TDOA measurements are generated according to (6.18) with $n_{i,j}$'s being Gaussian noises. $W$ is set to $W = \sigma^2 I$ with $\sigma = 1$. $\gamma$ is set to 1. The initial point for the WLSE is always set as the center of the deployment area.

Here we consider the scenario in which each cluster head exchanges its local measurements with its neighboring cluster heads to perform a local estimate, and then exchanges its local estimate with its neighboring cluster heads to perform diffusion until convergence. $C$ is set to

$$c_{i,k} = \begin{cases} \check{c}_{l,k}, & [t]_i \text{ involves cluster head } l, l \in N_k \text{ and } l \neq k \\ \check{c}_{k,k}, & [t]_i \text{ involves cluster head } k \\ 0, & \text{otherwise} \end{cases} \tag{6.31}$$

where

$$\check{c}_{l,k} = \begin{cases} 1/\max\{\deg_l, \deg_k\}, & l \in N_k,\ l \neq k \\ 1 - \sum_{l \neq k} \check{c}_{l,k}, & l = k \\ 0, & \text{otherwise.} \end{cases} \tag{6.32}$$

Here, $\check{c}_{l,k}$ denotes the weight assigned with respect to cluster heads $l$ and $k$, and $c_{i,k}$ represents the weight assigned to the $i$th measurement used by the cluster head $k$.

First, we fix $N = 16$ and vary the value of $M$, which changes from 5 to 50 with a step size of 5. The RMSEs of respective algorithms are shown in Fig. 6.7. It can be observed that *Global* is the best which can attain the CRLB, *local* is the worst and *Diff (con)* is always better than *local*. In general, *Diff (opt)* is better than *Diff (wei)*, and *Diff (wei)* is better than *Diff (con)*. The performance improvement of *Diff (opt)* and *Diff (wei)* compared with *Diff (con)* comes from the consideration of the reliability of the local estimates. Though the diffusion algorithms are always worse than *Global*, the performance differences are not significant. As $M$ grows, all the algorithms perform better.

Fig. 6.8 shows the corresponding average CPU times of respective algorithms except *Diff (opt)* whose CPU time is typically 10 times that of *Global* due to its numerical optimization nature (the same below). It can be seen that *Diff (con)* is very time efficient with a CPU time almost the same as *local*. *Diff (wei)* consumes a little more CPU time than *Diff (con)*, while the CPU time of *Global* is much larger. This demonstrates the advantage of the diffusion algorithm in terms of CPU time and computational complexity. Furthermore, we can say the diffusion algorithm has lower communication cost and computation complexity than the centralized solution, while the localization accuracy is close to the centralized method.

Fig. 6.9 shows the average number of iterations before convergence of the three diffusion algorithms. We can observe that *Diff (opt)* requires many fewer iterations compared with *Diff (con)* and *Diff (wei)*. *Diff (wei)* needs slightly more iterations than *Diff (con)*, which may explain our observation of a slightly longer CPU time consumed by *Diff (wei)*.

Then we examine the effect of $\sigma$ on the performance of the algorithms. We set $N = 16$ and $M = 10$. The RMSEs of respective algorithms are shown in Fig. 6.10. The relative performance of respective algorithms is the same as before. As $\sigma$ enlarges, all of them show performance degradation. The average CPU times and average number of iterations among different algorithms have the same relationship as before and thus the figures are not shown here.

Finally, we examine the choice of $\gamma$ on the performance of *Diff (wei)*. We set $N = 16$, $M = 10$ and $\sigma = 1$. We generate 200 realizations of the overall TDOA measurement vector, then store and use them for all the corresponding simulations. The corresponding RMSEs are shown in Fig. 6.11. It can be seen that an optimal $\gamma$ exists which results in the minimum RMSE for *Diff*

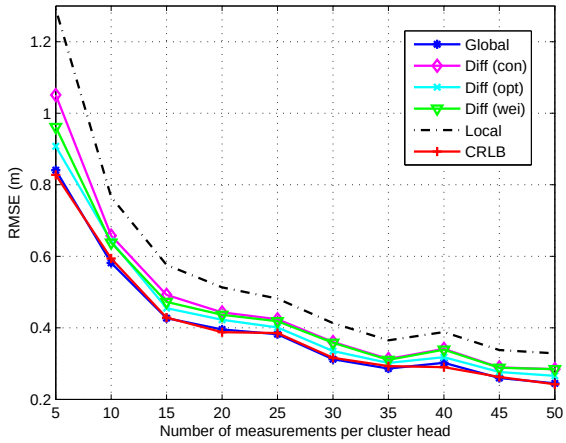


FIGURE 6.7: RMSE versus $M$ when $N = 16$.

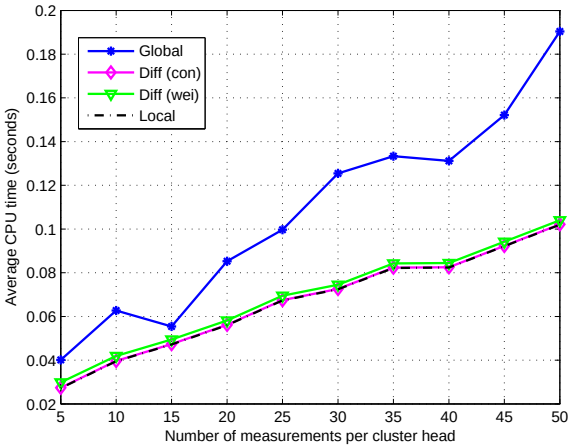


FIGURE 6.8: CPU time versus $M$ when $N = 16$.

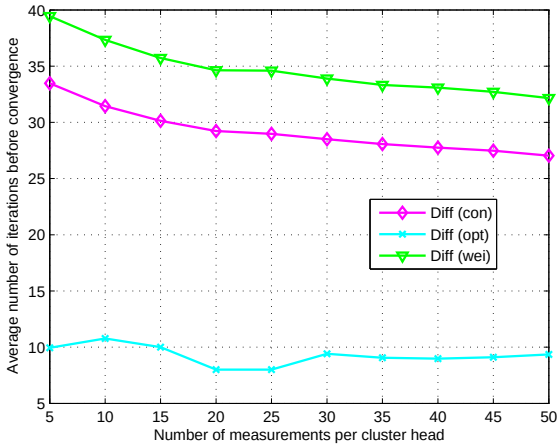


FIGURE 6.9: Average number of iterations before convergence versus $M$ when $N = 16$.

*(wei)*. However, in a large range of the choice of $\gamma$, *Diff (wei)* can generate better results than

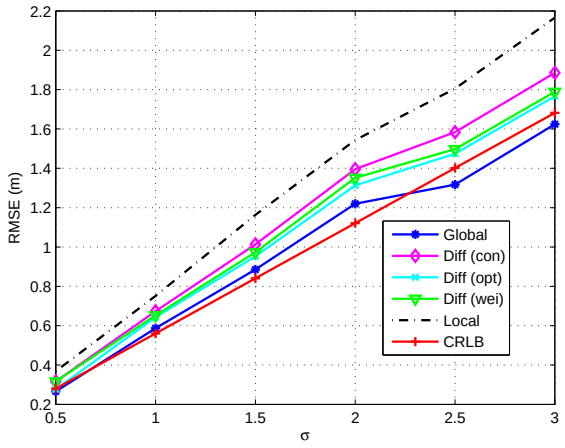


FIGURE 6.10: RMSE versus $\sigma$.

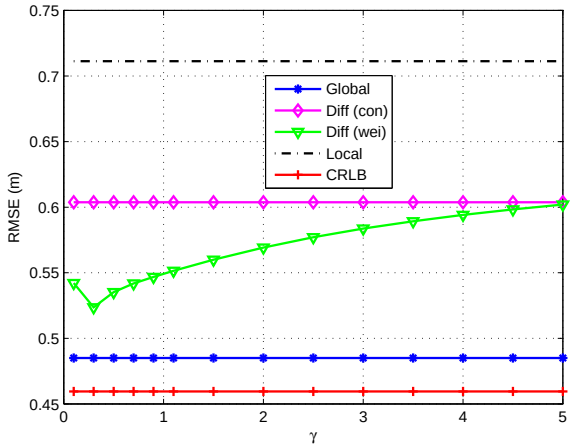


FIGURE 6.11: RMSE versus $\gamma$.

*Diff (con)*.

## 6.5 Summary

We have presented energy efficient localization schemes that can achieve high localization accuracy in wireless underground sensor networks. These distributed localization algorithms require low computational complexity and energy consumption based on a diffusion strategy. An accurate RCRT based ranging scheme using TDOA to determine range differences between sensors and source that does not require time synchronization is also proposed. It has been shown via simulation results that the proposed localization algorithms achieve excellent localization accuracy with lower communication cost. In future work, we plan to implement our localization scheme in a testbed and verify its performance with an actual WUSN.

# Chapter 7

# Conclusions and Future Work

The theme of this thesis is to study node localization in wireless sensor networks. We have proposed a series of novel approaches. Simulation results validate the effectiveness of our approaches. In this chapter, we summarize our work and point out some potential research directions.

## 7.1 Conclusions

Many localization algorithms have been developed and used to find the position of sensors. Although a lot of algorithms are proposed, it is still difficult to estimate the node location accurately and efficiently in WSN since the proposed algorithm should be with low complexity to reduce the communication cost for WSN. In this thesis, we studied the localization algorithm, especially focus on utilizing the statistical signal processing theory and techniques to derive accurate, robust and computationally attractive WSN positioning algorithms. The bias and variance performance measures of the developed algorithms are also produced.

- In Chapter 3, we present a range-free localization technique based on the radical line of intersecting circles. This technique provides greater accuracy than the centroid algorithm, at the expense of a slight increase in computational load. Simulation results show that for the scenarios studied, the radical line method can give an approximately 2 to 30% increase in accuracy over the centroid algorithm, depending on whether or not the anchors have identical ranges, and on the value of DOI.
- In Chapter 4, we have presented a new cooperative localization scheme that can achieve high localization accuracy in mobility-assisted wireless sensor networks when obstacles exist. Considering the complex localization scenario, namely, the feasible set is empty, a convex localization algorithm has been presented to address the effects of non-ideal

transmission of radio signals. We have developed an optimal movement schedule for MEs that can achieve a shortest path under expected localization accuracy. It has been shown in the simulation results that the proposed cooperative localization scheme can achieve high localization accuracy by including a mobile element.

- In Chapter 5, We present a distributed hop distance measurement and particle filter-based cooperative localization algorithm for mobile WSNs. Our proposal is scalable, robust, and self-adaptive to the dynamics of a mobile sensor network. Our proposed algorithm can reduce the hop distance estimation error accumulated over multiple hops by using a differential error correction scheme. In order to efficiently suppress redundant broadcasts and to reduce communication overhead, a backoff-based broadcast mechanism is proposed. It also improves localization performance by including particle filtering technology. Simulation results show that the proposed algorithm achieves better performance than other state-of-the-art algorithms.

- In Chapter 6, We have presented energy efficient localization schemes that can achieve high localization accuracy in wireless underground sensor networks. These distributed localization algorithms require low computational complexity and energy consumption based on a diffusion strategy. An accurate RCRT based ranging scheme using TDOA to determine range differences between sensors and source that does not require time synchronization is also proposed. It has been shown via simulation results that the proposed localization algorithms achieve excellent localization accuracy with lower communication cost.

## 7.2 Future Work

An unknown-position sensor can be localized if there are three or more anchors making time-of-arrival (TOA) measurements of a signal from it. However, the location errors can be very large due to the fact that some of the measurements are from non-line-of-sight (NLOS) paths. In the future, we will propose a semi-definite programming (SDP) based node localization algorithm in NLOS environment for ultra-wideband (UWB) wireless sensor networks. The positions of sensors can be estimated using the distance estimates from location-aware anchors as well as other sensors. However, in the absence of line-of-sight (LOS) paths, e.g., in indoor networks, the NLOS range estimates can be significantly biased. As a result, the NLOS error can remarkably decrease the location accuracy, and it is not easy to accurately distinguish the LOS from NLOS measurements. According to the information known about the prior probabilities and distributions of the NLOS errors, three different cases will be introduced and the related localization problems will be addressed respectively in the future work.

Anchor based approaches requires of a set of anchor nodes with known positions and the distribution for anchors. Hence, an optimal as well as robust scheme will be to have a minimum number of beacons in a region and find the optimal distribution for anchors. Further work is required to find the minimum number of anchors and the optimal distribution to find each node's position with a higher accuracy.

It is also very important to verify our algorithms via real testbeds in our future work.

# List of Publication

## International Journal Papers

1. Hongyang Chen, Kaoru Sezaki, Ping Deng, and Hing Cheung So, An Improved DV-Hop Localization algorithm with reduced location error for WSNs, *IEICE Transactions on Fundamentals*, vol. E91-A, no. 8, pp. 2232-2236, August 2008.

2. Hongyang Chen, Q. Shi, P. Huang, H. Vincent Poor, and K. Sezaki, Mobile Anchor Assisted Node Localization for Wireless Sensor Networks, *IEEE Trans. on Wireless Communications*, Vol. 9, No. 3, pp. 956-963, Mar. 2010.

## International Conference Papers

1. Hongyang Chen, Kaoru Sezaki, Ping Deng, and Hing Cheung So, An improved DV-hop localization algorithm for wireless sensor networks, In *Proc. IEEE Conference on Industrial Electronics and Applications (ICIEA 2008)*, pp.1557-1561, June 2008, Singapore.

2. Hongyang Chen, P. Huang, M. Martins, H.C. So, and K. Sezaki, Novel centroid localization algorithm for three-dimensional wireless sensor networks, In *Proc. 4th International Conference on WirelessCommunications, Networking and Mobile Computing (WiCOM 2008)*, Oct. 2008, Dalian, China.

3. Hongyang Chen, P. Huang, H.C. So, and K. Sezaki, Mobility-assisted position estimation in wireless sensor networks, In *Proc. 14th IEEE International Conference on Parallel and Distributed Systems (ICPADS 2008)*, pp.607-614, December 2008, Melbourne, Victoria, Australia.

4. Hongyang Chen, M.H.T. Martins, P. Huang, H.C. So, and K. Sezaki, Cooperative node localization for mobile sensor networks, In *Proc. 2008 International Conference On Embedded and Ubiquitous Computing (EUC 2008)*, vol.I, pp.302-308, December 2008, Shanghai, China.

5. Hongyang Chen, Q. Shi, P. Huang, H. Vincent Poor, and K. Sezaki, Mobile Anchor Assisted Node Localization for Wireless Sensor Networks, In *Proc. IEEE PIMRC'09*, Sept. 2009, Tokyo, Japan.

6. Hongyang Chen, Y.T. Chan, H. Vincent Poor, and K. Sezaki, Range-free Localization with Radical Line, In *Proc. IEEE ICC'10*, May, 2010, Cape Town, South Africa.

## Other Publications

1. Pei Huang, Hongyang Chen, Guoliang Xing, and Yongdong Tan, SGF: A State-Free Gradient-Based Forwarding Protocol for Wireless Sensor Networks, *ACM Transactions on Sensor Networks (TOSN)*, Vol. 5, No. 2, Mar. 2009.

2. Q. Shi, C. He, Hongyang Chen, and L. Jiang, Distributed Wireless Sensor Network Localization via Sequential Greedy Optimization Algorithm, *IEEE Transactions on Signal Processing*, Vol. 58, No. 6, pp. 3328-3340, Jun. 2010.

3. B. Liu, Hongyang Chen, X. Lei, F. Ren, and K. Sezaki, Internode Distance-Based Redundancy Reliable Transport in Underwater Sensor Networks, *EURASIP Journal on Wireless Communications and Networking*, 2010.

4. B. Liu, F. Ren, J. Shen, and Hongyang Chen, Advanced Self-Correcting Time Synchronization in Wireless Sensor Networks, *IEEE Communications Letters*, Vol. 14, No. 4, pp. 309-311, Apr. 2010.

5. B. Liu, Hongyang Chen, Z. Zhong, and H. V. Poor, Asymmetrical Round Trip Based Synchronization-free Localization in Large-scale Underwater Sensor Networks, *IEEE Transactions on Wireless Communications*, Vol. 9, No. 11, pp 3532-3542, November 2010.

6. J. Wang, Q. Gao, H. Wang, Hongyang Chen, and M. Jin, Robust tracking algorithm for wireless sensor networks based on improved particle filter, *Wireless Communications and Mobile Computing*, Aug. 2010.

# Bibliography


[1] Telosb datasheet, crossbow technology inc.

[2] A. Baggio and K. Langendoen. Monte Carlo localization for mobile wireless sensor networks. *Ad Hoc Netw.*, 6(5):718–733, 2008.

[3] P. Biswas, T.-C. Lian, T.-C. Wang, and Y. Ye. Semidefinite programming based algorithms for sensor network localization. *TOSN*, 2(2):188–220, 2006.

[4] S. Biswas and R. Morris. ExOR: opportunistic multi-hop routing for wireless networks. *SIGCOMM Comput. Commun. Rev.*, 35(4):133–144, 2005.

[5] A. Bletsas, A. Khisti, D. P. Reed, and A. Lippman. A simple cooperative diversity method based on network path selection. *IEEE Journal on Selected Areas in Communications*, 24(3):659–672, 2006.

[6] S. Boyd and L. Vandenberghe. *Convex Optimization.* Cambridge University Press, Cambridge, UK, 2004.

[7] P. Brass. Bounds on coverage and target detection capabilities for models of networks of mobile sensors. *ACM Trans. on Sensor Netw.*, 3(2):9, 2007.

[8] N. Bulusu, J. Heidemann, and D. Estrin. Gps-less low cost outdoor localization for very small devices. *IEEE Personal Comm. Magazine*, 7(5):28–34, 2000.

[9] T. Camp, J. Boleng, and V. Davies. A survey of mobility models for ad hoc network research. *Wireless Communications & Mobile Computing (WCMC): Special Issue on Mobile Ad Hoc Networking: Research, Trends and Applications*, 2:483–502, 2002.

[10] F. S. Cattivelli, C. G. Lopes, and A. H. Sayed. Diffusion recursive least-squares for distributed estimation over adaptive networks. *IEEE Transactions on Signal Processing*, 56(5):1865–1877, 2008.

[11] Y. Chan, T. Lo, and H. So. Passive range-difference estimation in a dispersive medium. *IEEE Transactions on Signal Processing*, 58(3):1433–1439, 2010.

[12] H. Chen, K. Sezaki, P. Deng, and H. C. So. An improved dv-hop localization algorithm with reduced location error for wsns. *IEICE Transactions on Fundamentals*, E91-A:2232–2236, Aug. 2008.

[13] H. S. M. Coxeter. *Introduction to Geometry.* New York: Wiley, 1969.

[14] K. Dantu, M. H. Rahimi, H. Shah, S. Babel, A. Dhariwal, and G. S. Sukhatme. Robomote: enabling mobility in sensor networks. In *IPSN*, pages 404–409, 2005.

[15] B. Dil, S. Dulman, and P. Havinga. Range-based localization in mobile sensor networks. *Lecture Notes in Computer Science*, 3868:164–179, 2006.

[16] D. Dong, Y. Liu, and X. Liao. Fine-grained boundary recognition in wireless ad hoc and sensor networks by topological methods. In *MobiHoc*, pages 135–144, 2009.

[17] A. Gallo, F. Malucelli, and M. Marre. Hamiltonian paths algorithms for disk scheduling. *Technical Report 20/94*, 1994.

[18] G. Giorgetti, S. K. S. Gupta, and G. Manes. Wireless localization using self-organizing maps. In *IPSN*, pages 293–302, 2007.

[19] T. He, C. Huang, B. M. Blum, J. A. Stankovic, and T. F. Abdelzaher. Range-free localization schemes for large scale sensor networks. In *MOBICOM*, pages 81–95, 2003.

[20] M. Heissenbüttel, T. Braun, T. Bernoulli, and M. Wälchli. BLR: beacon-less routing algorithm for mobile ad-hoc networks. *Elsevier's Computer Communications Journal (Special Issue)*, 27:1076–1086, 2004.

[21] Y.-L. Hsieh and K. Wang. Efficient localization in mobile wireless sensor networks. In *SUTC '06: Proc. of IEEE International Conference on Sensor Networks, Ubiquitous, and Trustworthy Computing*, pages 292–297, Washington, DC, USA, 2006.

[22] L. Hu and D. Evans. Localization for mobile sensor networks. In *Proc. of ACM MobiCom*, pages 45–57, New York, NY, USA, 2004.

[23] S. M. Kay. *Fundamentals of Statistical Signal Processing: Estimation Theory.* Englewood Cliffs, NJ: Prentice-Hall, 1993.

[24] S. Lederer, Y. Wang, and J. Gao. Connectivity-based localization of large-scale sensor networks with complex shape. *TOSN*, 5(4), 2009.

[25] J. X. Lee, Z. W. Lin, P. S. Chin, and C. L. Law. The use of symmetric multi-way two phase ranging to compensate time drift in wireless sensor network. *IEEE Transactions on Wireless Communications*, 8(2):613–616, 2009.

[26] G. Li, J. Xu, Y.-N. Peng, and X.-G. Xia. An efficient implementation of robust phase-unwrapping algorithm. *IEEE Signal Process. Lett.*, 14.

[27] M. Li and Y. Liu. Rendered path: range-free localization in anisotropic sensor networks with holes. *IEEE/ACM Trans. Netw.*, 18(1):320–332, 2010.

[28] X. Li, H. Liang, and X. Xia. A robust chinese remainder theorem with its applications in frequency estimation from undersampled waveforms. *IEEE Transactions on Signal Processing*, 57(14):4314–4322, 2010.

[29] Z. Li, W. Dehaene, and G. G. E. Gielen. A 3-tier uwb-based indoor localization system for ultra-low-power sensor networks. *IEEE Transactions on Wireless Communications*, 8(6):2813–2818, 2009.

[30] K. W.-K. Lui, W.-K. Ma, H.-C. So, and F. K. W. Chan. Semi-definite programming algorithms for sensor network node localization with uncertainties in anchor positions and/or propagation speed. *IEEE Transactions on Signal Processing*, 57(2):752–763, 2009.

[31] J. Luo, H. V. Shukla, and J.-P. Hubaux. Non-interactive location surveying for sensor networks with mobility-differentiated toa. In *INFOCOM*, 2006.

[32] D. Lymberopoulos and A. Savvides. Xyz: a motion-enabled, power aware sensor node platform for distributed sensor network applications. In *IPSN*, pages 449–454, 2005.

[33] T. Moscibroda, R. Wattenhofer, and A. Zollinger. Topology control meets sinr: The scheduling complexity of arbitrary topologies. In *MobiHoc*, pages 310–321, 2006.

[34] R. Nagpal, H. Shrobe, and J. Bachrach. Organizing a global coordinate system from local information on an ad hoc sensor network. *Lecture Notes in Computer Science*, 2634:333–348, 2003.

[35] D. Niculescu and B. Nath. Ad hoc positioning system (APS). In *Proc. of IEEE GLOBECOM*, volume 5, pages 2926–2931, Nov. 2001.

[36] K. Römer. The lighthouse location system for smart dust. In *MobiSys*, 2003.

[37] C. Savarese, J. M. Rabaey, and K. Langendoen. Robust positioning algorithms for distributed ad-hoc wireless sensor networks. In *USENIX Annual Technical Conference, General Track*, pages 317–327, 2002.

[38] M. Sha, G. Xing, G. Zhou, S. Liu, and X. Wang. C-mac: Model-driven concurrent medium access control for wireless sensor networks. In *INFOCOM*, pages 1845–1853, 2009.

[39] Y. Shang, W. Ruml, Y. Zhang, and M. P. J. Fromherz. Localization from mere connectivity. In *MobiHoc*, pages 201–212, 2003.

[40] Q. Shi, C. He, H. CheN, and L. Jiang. Distributed wireless sensor network localization via sequential greedy optimization algorithm. *IEEE Transactions on Signal Processing*, 58(6):3328–3340, 2010.

[41] Q. Shi, C. He, L. ge Jiang, and J. Luo. Sensor network localization via nondifferentiable optimization. In *GLOBECOM*, pages 12–16, 2008.

[42] A. Silva and M. Vuran. Communication with aboveground devices in wireless underground sensor networks: An empirical study. In *Proc. ICC'10*, 2010.

[43] A. R. Silva and M. C. Vuran. Empirical evaluation of wireless underground-to-underground communication in wireless underground sensor networks. In *DCOSS*, pages 231–244, 2009.

[44] A. R. Silva and M. C. Vuran. Development of a testbed for wireless underground sensor networks. *EURASIP Journal on Wireless Communications and Networking*, 2010.

[45] A. A. Somasundara, A. Ramamoorthy, and M. B. Srivastava. Mobile element scheduling with dynamic deadlines. *IEEE Trans. Mob. Comput.*, 6(4):395–410, 2007.

[46] K.-F. Ssu, C.-H. Ou, and H. C. Jiau. Localization with mobile anchor points in wireless sensor networks. *IEEE Trans. Veh. Technol.*, 54(3):1187–1197, 2005.

[47] R. Stoleru, T. He, J. A. Stankovic, and D. P. Luebke. A high-accuracy, low-cost localization system for wireless sensor networks. In *SenSys*, pages 13–26, 2005.

[48] T. Stoyanova, F. Kerasiotis, A. S. Prayati, and G. D. Papadopoulos. Evaluation of impact factors on rss accuracy for localization and tracking applications. In *MOBIWAC*, pages 9–16, 2007.

[49] E. Stuntebeck, D. Pompili, and T. Melodia. Underground wireless sensor networks using commodity terrestrial motes. In *Proc. IEEE SECON'06*, pages 112–124, 2006.

[50] J. F. Sturm. Using SEDUMI 1.02, a MATLAB* toolbox for optimization over symmetric cones, 2001. Downloadable from http://sedumi.mcmaster.ca.

[51] Z. Sun and I. F. Akyildiz. Connectivity in wireless underground sensor networks. In *Proc. SECON*, pages 1–9, 2010.

[52] V. Vivekanandan and V. W. S. Wong. Concentric anchor-beacons localization algorithm for wireless sensor networks. *IEEE Trans. Veh. Technol.*, 56(5):2733–2745, 2007.

[53] C. Wang and L. Xiao. Sensor localization in concave environments. *TOSN*, 4(1), 2008.

[54] D. Wang, J. Liu, and Q. Zhang. Mobility-assisted sensor networking for field coverage. In *GLOBECOM*, pages 1190–1194, 2007.

[55] G. Wang, G. Cao, and T. F. L. Porta. Movement-assisted sensor deployment. In *INFOCOM*, 2004.

[56] G. Wang, M. J. Irwin, P. Berman, H. Fu, and T. F. L. Porta. Optimizing sensor movement planning for energy efficiency. In *ISLPED*, pages 215–220, 2005.

[57] W. Wang, V. Srinivasan, B. Wang, and K. C. Chua. Coverage for target localization in wireless sensor networks. *IEEE Transactions on Wireless Communications*, 7(2):667–676, 2008.

[58] A. J. Weiss and J. S. Picard. Network localization with biased range measurements. *IEEE Transactions on Wireless Communications*, 7(1):298–304, 2008.

[59] B. Xiao, H. Chen, and S. Zhou. Distributed localization using a moving beacon in wireless sensor networks. *IEEE Trans. Parallel Distrib. Syst.*, 19(5):587–600, 2008.

[60] G. Xing, J. Wang, K. Shen, Q. Huang, X. Jia, and H.-C. So. Mobility-assisted spatiotemporal detection in wireless sensor networks. In *ICDCS*, pages 103–110, 2008.

[61] F. Ye, A. Chen, S. Lu, and L. Zhang. A scalable solution to minimum cost forwarding in large sensor networks. In *ICCNC: Proc. of the 10th International Conference on Computer Communications and Networks*, pages 304–309, 2001.

[62] D. Zhang, J. Ma, Q. Chen, and L. M. Ni. An rf-based system for tracking transceiver-free objects. In *PerCom*, pages 135–144, 2007.

[63] W. Zhang, Q. Yin, X. Feng, and W. Wang. Distributed tdoa estimation for wireless sensor networks based on frequency-hopping in multipath environment. In *VTC Spring*, pages 1–5, 2010.

[64] M. Zuniga and B. Krishnamachari. Analyzing the transitional region in low power wireless links. In *Proc. SECON'04*, pages 517–526, Santa Clara, CA, 2004.